

1  
2 **Progress and potential of metal-organic frameworks (MOFs) as**  
3 **novel desiccants for built environment control: a review**

4 Kan Zu, Menghao Qin\*, Shuqing Cui

5 Department of Civil Engineering, Technical University of Denmark, Lyngby, Denmark

6 \* Corresponding author details, [menqin@byg.dtu.dk](mailto:menqin@byg.dtu.dk)

7  
8 **Abstract:** The regulation of the balance of the sensible and latent loads remains a critical  
9 problem for built environment control. Unlike the traditional vapor compression system that  
10 features high-energy consumption and environmental-unfriendly processes, desiccants  
11 represent an alternative air-conditioning method that takes advantage of the low-grade energy,  
12 decreases the energy consumption and even employs use of water vapor. Though the desiccant-  
13 based systems can achieve spatial moisture transfer through the periodic adsorption/desorption  
14 process, however, the water-stable desiccants with high water uptake and mildly reversible  
15 adsorption are required, and the traditional desiccants cannot meet these requirements. In this  
16 respect, metal-organic frameworks (MOFs), possessing a variety of structures and precise  
17 functional ability to optimize their properties, are promising porous materials exhibiting high  
18 potential for rational design and sorption-based applications. In this review, intrinsic properties  
19 and prevalent water adsorption mechanisms of the potential micro/mesoporous MOF  
20 desiccants have been elucidated. Subsequently, the selection criteria of the promising MOF  
21 desiccants for water loading removal from air in the built environment is proposed and some  
22 currently available water-stable MOFs based on different working humidity ranges have been  
23 analyzed for the potential humidity control from the aspects of microstructure, isotherms and  
24 regeneration conditions. Finally, approaches for screening the well-suited MOFs from material  
25 and system levels is presented. Overall, the cases of actual applications in the active or passive

26 way have confirmed that MOF-based systems can effectively regulate the humidity load within  
27 the desirable range, thus, underlining the high potential of large-scale applications in the near  
28 future.

29

30 ***Highlights:***

31 1 . Research on metal-organic framework (MOF) materials for the built environment control  
32 has been reviewed.

33 2 . Special crystal structure of MOF plays an important role in the adsorption mechanism.

34 3 . The selection criteria and classification of MOFs disclose the potential application in solid  
35 desiccant systems.

36 4 . Developments of MOF commercialization and system-related technologies (i.e. coating  
37 process) are prospected.

38

39 ***Keywords:*** MOFs, intrinsic properties, adsorption mechanism, screening, active/passive-type,  
40 solid desiccant system

41

42 **Word count** (excluding title, author names and affiliations, keywords, abbreviations,  
43 table/figure captions, acknowledgments and references): **9995**

## 44 **1. Introduction**

45 Benefitting from the scientific inventions of the contemporary era, people's lifestyle has  
46 evolved from early open-air living spaces into more comfortable and enclosed air-conditioned  
47 ones. The energy consumption by the air conditioning systems represents more than 40% of  
48 the total building energy consumption. In the traditional cooling dehumidification, the cooling  
49 air below the dew point, used to remove both sensible and latent loads, gives rise to a large  
50 extent of energy waste owing to the low trigger temperature for the latent load removal [1, 2].  
51 Therefore, the critical problem in the indoor air-conditioned zones is to achieve an independent  
52 control of temperature and humidity [3, 4]. It is to be noted that either moisture accumulation  
53 or deficiency will cause discomfort to human beings and damage to building materials, and  
54 45%~65% relative humidity (RH) in residential buildings has been recommended by the  
55 American Society of Heating, Refrigerating and Air-Conditioning Engineers (ASHRAE) [5].  
56 In this regard, the introduction of desiccant materials is an alternative method to achieve  
57 effective humidity control within a desirable range, and extensive studies have been devoted to  
58 the synthesis and application of new desiccants possessing high water capacity and gentle  
59 regeneration conditions [6, 7].

60

61 Desiccants can generally be classified into liquid and solid phase. As the liquid desiccant  
62 dehumidifiers suffer from large and complicated systems, metal corrosion, etc., the solid  
63 desiccant systems (SDSs) progressively exhibit potential as promising methods for indoor  
64 humidity control [8, 9]. Some commercially used materials, like zeolites and silica gels, have  
65 been incorporated into the air-conditioning systems, but these are incapable of achieving high-  
66 performance dehumidification due to the harsh regeneration condition or low work loading [10,  
67 11]. Therefore, research efforts are going for the development of novel solid desiccants with an  
68 ability to improve the whole system performance with respect to the built environment control.

69 Recently, micro- and mesoporous materials such as metal-organic frameworks (MOFs) have  
70 emerged as an effective alternative to the currently used desiccants [9]. The MOFs are  
71 constructed by the formation of strong chemical bonds to bridge inorganic metal-related units  
72 with organic ligands, thus, creating open frameworks with ordered structure [12, 13]. A high  
73 level of structural flexibility and ultra-high porosity make these materials promising desiccants  
74 in the sorption-based applications [14]. In addition, most of the MOFs have S-shaped isotherms  
75 with a steep rise in a narrow relative humidity (RH) range. The observed steep rise is directly  
76 correlated with the special adsorption mechanism of MOFs, however, it does not rely on the  
77 formation of strong bonding sites in the crystalline frameworks, thus, partly indicating their  
78 gentle regeneration condition [15].

79  
80 To date, more than 80000 different MOFs have been reported, but only a small number of  
81 literature studies have investigated their distinct advantages over traditional materials in the  
82 air-conditioning system [16, 17]. One critical challenge appears to be the effective screening  
83 of the available MOF desiccants. First, the long-term water stability is the precondition that  
84 ensures the conservation of their frameworks [10]. Hydrothermal stability tests over several  
85 thousands of adsorption/ desorption cycles have been proven only for a few structures [18-21],  
86 while most reports have presented only a few dozen cycles on laboratory scale. Second, the  
87 working performance (adsorption and desorption) of MOF desiccants is of importance for the  
88 working efficiency. At present, a small number of studies have been reported on the MOF-  
89 based open SDSs (directly contacting the ambient air) for humidity regulation in buildings.  
90 However, water-harvesting applications [22-24] and explorations of the sorption-based close  
91 SDSs (without contacting the ambient air) such as heat pumps [25-31] and adsorption-based  
92 refrigeration [20, 32-34] provide more information about the basic hydrothermal properties of  
93 MOFs. Third, the intrinsic properties of the MOF chemicals decide the application area. In

94 general, it is also preferred to use green and safe materials with low cost in the practical  
95 applications [35]. Besides, the other challenge is to classify the MOF desiccants. In general,  
96 MOFs such as MOF-801 [36], MOF-841 [37], MIL-160 [25], CAU-10 [38], Co<sub>2</sub>Cl<sub>2</sub>(BTDD)  
97 [39], etc., have been investigated for good working capacity in the 0~30% RH range, while  
98 MIL-100 (Cr, Fe, Al) [27, 40], MIL-101(Cr) [41], Cr-**soc**-MOF-1 [42], Y-**shp**-MOF-5 [21],  
99 UiO-66 [37], etc., exhibit high working capacity in the 30%~65% RH range. Especially, Y-  
100 **shp**-MOF-5 [21] and Cr-**soc**-MOF-1[42] demonstrate autonomous humidity control within a  
101 desirable range (45%~65% RH) for the building environment. Thus, the ongoing work on the  
102 classification of MOFs should be intensively developed.

103

104 To the best of our knowledge, there are only a few comprehensive overviews focusing on MOFs  
105 for the water adsorption applications [16, 17, 43, 44], not to mention the built environment  
106 control. In this review, we will explore in detail the development of MOFs in built environment  
107 control from materials and systems. A brief review of the compositions and intrinsic properties  
108 of the MOF materials has been presented. Some basic selection criteria of MOFs for humidity  
109 load control have been subsequently proposed, and three groups of MOFs have been classified  
110 and discussed based on their different trigger point (a turning point  $P/P_0$  before a steep rise in  
111 isotherms). At the end of this review, the strategy and design of systems using MOF materials  
112 have been provided for either passive or active methods. Though it is hard to review the vast  
113 number of literature studies on MOFs and make a well-considered evaluation on this subject,  
114 it is still hoped that the review provides some insights into the selection of the most suitable  
115 MOFs depending on the different conditions with reference to their application in the built  
116 environment control.

117

118

## 119 **2. Compositions and intrinsic properties of MOFs**

### 120 2.1. Compositions

121 A specific MOF requires the provision of metal ions derived from the inorganic metal salts,  
122 organic ligands, and possibly solvents. MOFs with desirable structures can be prepared through  
123 the component exchanges in the metal ions, ligands or solvents.

124

125 Metal ions: metal-containing units are used for bonding with organic groups. To date, many  
126 metal ions have been reported for developing MOFs with high hydrolytic stability, most of  
127 which traditionally are divalent metal ions such as  $\text{Cu}^{2+}$ ,  $\text{Zn}^{2+}$ ,  $\text{Zr}^{2+}$ ,  $\text{Ni}^{2+}$ ,  $\text{Co}^{2+}$ ,  $\text{Mg}^{2+}$  and  $\text{Cd}^{2+}$   
128 [30, 39, 45-47], trivalent metal ions such as  $\text{Fe}^{3+}$ ,  $\text{Cr}^{3+}$  and  $\text{Al}^{3+}$  [27], and even tetravalent ions  
129 such as  $\text{Ti}^{+4}$  and  $\text{Hf}^{+4}$  [48, 49]. In past decades, many studies have also been conducted on  
130 lanthanide series (i.e., Ce, Pr and Eu), p-block elements (i.e., Ga and In) and even mix-metals  
131 [10, 50, 51].

132 Ligands (linkers): the ligands are used to connect the metal clusters, which shape the crystal  
133 framework. The structure of ligands can provide insights about the hydrophilicity/  
134 hydrophobicity of the pore surface. Theoretically, longer ligands bear larger surface area, thus,  
135 providing more adsorption sites and storage space, and correspondingly affecting the  
136 adsorption capacity. Common ligands used in the synthesis of water-stable MOFs include BTC  
137 (1, 3, 5-benzene tricarboxylic acid), TPA (terephthalic acid), TDC (thiophene-2, 5-dicarboxylic  
138 acid), fumaric acid, etc. [40, 41, 49].

139 Solvents: the solvents are not a necessity during the synthesis of MOFs, especially for  
140 mechanochemical synthesis. However, the solvents can provide a benign environment for the  
141 chemical reactions, resulting in the diversity of the formed structures. Besides, the solvents can  
142 also determine the thermodynamics and activation energy for a specific reaction. The  
143 commonly used solvents are water and organic solvents such as ethanol, acetone and ethyl

144 acetate. A few non-green solvents (e.g. dimethyl sulfoxide, tetrahydrofuran, toluene, formic  
145 acid etc.) can also be used in the large-scale production by strictly following the standard  
146 procedures [52, 53].

147

## 148 2.2. Intrinsic properties

149 The remarkable performance of MOFs has advanced their synthesis, accompanied by the  
150 development of geometric topology design, post-synthetic modification and multivariate  
151 MOFs. It is to be noted that the interaction between the acceptor and target pairs (i.e. MOF-  
152 water vapor) makes the MOFs competent desiccants. Namely, the intrinsic properties of MOFs  
153 drive the performance for water uptake and corresponding applications (Table 1 and Table 2).

154

### 155 2.2.1. Metal sites

156 There are many coordinatively unsaturated metal sites inside the MOF structure, where the  
157 guest molecules such as water or other organic solvents can be coordinated after synthesis [54].  
158 Prior to the practical usage, activation is needed to help remove these guest molecules from the  
159 metal nodes by heating in a vacuum environment. As the exposed sites exhibit strong polarity,  
160 MOFs demonstrate relatively high affinity towards vapor molecules even at low vapor pressure.  
161 Correspondingly, the amount of the recovered unsaturated metal sites can enhance the  
162 adsorption capacity of MOFs for vapor molecules [55, 56].

163

### 164 2.2.2. Functionality and expansion of structures

165 Apart from metal sites, the combination of functional groups with ligands is also an alternative  
166 to improve the hydrophobicity/ hydrophilicity of MOF chemicals, tune the shape of isotherms  
167 or move their trigger points ( $P/P_0$ ). Commonly used hydrophilic functional groups, such as -  
168  $\text{NO}_2$  (nitro),  $-\text{NH}_2$  (amino),  $-\text{OH}$  (hydroxyl), etc., have been reported for the synthesis of MOFs

169 [57-62]. In comparison with the original MOFs without functionalities, the functionalized  
170 MOFs demonstrate strong tunability in isotherms, however, at the expense of surface area or  
171 pore volume. On the other hand, the exploitation of MOF-based composite materials has also  
172 gained interest. In order to facilitate the heat and mass transfer of desiccants, MOFs have also  
173 been combined with inorganic salts or carbon substrates to improve the adsorption performance.  
174 For instance,  $\text{CaCl}_2@\text{UiO-66}$  and  $\text{MIL-101}(\text{Cr})@\text{graphene oxide}$  have been reported to  
175 possess high water capacity [63-67].

176  
177 In addition, a few research studies have expanded the MOF structures based on the same  
178 topology, which indicates that it is possible to develop identically topological and uniquely  
179 functional MOFs. An example of such cases is HKUST-1 [ $\text{Cu}_3(\text{BTC})_2$ ], which results from the  
180 bridging of copper metal ions ( $\text{Cu}^{2+}$ ) with tritopic ligand ( $\text{BTC}^{3-}$ ). Identically topological  
181 structures were constructed through ligand expansion from BTC to TATB, and further to BBC.  
182 The BBC analog has been reported to possess 17.4 times volume as compared to the original  
183 HKUST-1 [68]. Accordingly, the developed extension exhibits the potential to provide more  
184 adsorption sites for achieving diverse functionalities.

185

### 186 2.2.3. Porosity, surface area and pore apertures

187 From the perspective of topology, MOFs consist of the units of nodes (metal ions) and rods  
188 (ligands), and the rods generally encompass a number of void spaces therefore making MOFs  
189 porous materials. To date, the flexibility of the selection of both metal ion sources and organic  
190 ligands has resulted in various internal structures, leading to a wide range of surface area (from  
191 hundreds to thousands  $\text{m}^2/\text{g}$ ) and porosity up to 90% [69], with pore size in micropore range  
192 ( $\sim\text{nm}$ ) or even smaller [70]. Furthermore, according to the synthesis methods reported in  
193 literature, the reaction conditions have a direct correlation with the intrinsic structure through



194 the control on the residence time, feed mass, reaction temperature, etc., thus, allowing  
 195 flexibility during synthesis.

196

197 **Table 1**

198 Reported real applications of MOFs in water adsorption.

Materials	Surface area (m <sup>2</sup> g <sup>-1</sup> )	Pore Volume (cm <sup>3</sup> g <sup>-1</sup> )	Pore diameter (nm)	Uptake (g g <sup>-1</sup> )	P/P <sub>0</sub> of the steep adsorption	Possible regeneration condition	Refs.
CAU-10(Al)	635	0.43	0.7	0.36	0.15-0.25	70°C	[32, 38]
MIL-53-FA(Al)	1080	0.49	0.6	0.53	0.2-0.35	90°C	[52, 71]
MIL-100 (Fe)	1917	1.0	2.5/2.9	0.77	0.25-0.45	<70°C	[27, 72]
MOF-801(Zr)	990	0.45	0.48/0.5 6/0.77	0.36	0.05-0.15	80-85°C	[37, 73]
MOF-303(Al)	-	0.54	0.6	0.48	0.1-0.25	85°C	[22, 74]

199

200 **Table 2**

201 Promising MOFs in water adsorption applications.

Materials	Surface area (m <sup>2</sup> g <sup>-1</sup> )	Pore Volume (cm <sup>3</sup> g <sup>-1</sup> )	Pore diameter (nm)	Uptake (g g <sup>-1</sup> )	P/P <sub>0</sub> of the steep adsorption	Possible regeneration condition	Refs.
BIT-66(V)	1417	0.87	0.65/2.5 8	0.71	0.6	-	[75]
BUT-46A(Zr)	1550	0.69	1.6-3.5	0.52	0.44-0.49	-	[76]
BUT-46B(Zr)	1430	0.65	1.6-3.5	0.49	0.51-0.55	-	[76]
BUT-46F(Zr)	1563	0.71	1.6-3.5	0.59	0.39-0.43	-	[76]
BUT-46W(Zr)	1565	0.71	1.6-3.5	0.63	0.27-0.37	-	[76]
CAU-1(Al)	1300	0.55	0.5/1.0	0.55	0.38	-	[77]
CAU-23(Al)	1250	0.48	-	0.37	0.3	60°C	[20]
CUK-1(Co)	510	0.26	-	0.28	0.12	-	[30]

CUK-1(Mg)	580	0.28	-	0.36	0.23-0.28	-	[30]
CUK-1(Ni)	520	0.26	-	0.3	0.12	-	[30]
Cr-soc-MOF-1	4549	2.1	-	1.95	0.58-0.72	25°C, RH<45%	[42]
DUT-67(Hf)	810	0.33	-	0.29	0.25-0.45	-	[49]
DUT-67(Zr)	1064	0.44	-	0.41	0.25-0.45	-	[49]
DUT-68(Hf)	749	0.34	-	0.29	0.38-0.42	-	[49]
DUT-68(Zr)	891	0.41	0.8/1.3/ 1.4/2.8	0.34	0.38-0.42	-	[49]
DUT-69(Hf)	450	0.22	-	0.2	-	-	[49]
DUT-69(Zr)	560	0.31	-	0.26	-	-	[49]
MIL-100(Al)	1814	1.14	2.5/2.9	0.5	0.25-0.45	-	[27]
MIL-100 (Cr)	1517	-	2.5/2.9	0.8	0.25-0.42	-	[40]
MIL-101(Cr)	5900	2.0	2.9/3.4	-	-	-	[41]
	4150	-	-	>1.5	0.4-0.5	70°C	[78]
+NO <sub>2</sub> (Cr)	2146	1.19	<2.9/3.4	1.08	0.41-0.52	-	[57]
+NH <sub>2</sub> (Cr)	2509	1.27	<2.9/3.4	0.9	0.37-0.44	-	[57]
+SO <sub>3</sub> H(Cr)	1920	0.94	<2.9/3.4	0.62	0.28-0.36	-	[57]
MAF-7(Zn)	1870	0.67	-	0.43	0.26-0.3	-	[79]
MIL-160(Al)	1070	0.398	-	0.37	0.05-0.16	90°C	[25]
MIL-125- NH <sub>2</sub> (Ti)	1509	0.66	-	0.68	0.2	-	[48, 80]
MIP-200(Zr)	1000	0.4	-	0.46	0.17	65-70°C	[46]
MOF-74(Mg)	1250	0.53	1.11	0.75	0-0.05	-	[37]
MOF-808	2360	0.84	1.84	0.6	0.28-0.32	-	[37]
MOF-841(Zr)	1390	0.53	0.92	0.5	0.26	80°C	[37, 81]
Co <sub>2</sub> Cl <sub>2</sub> (BTDD )	1912	-	2.2	0.97	0.28	55°C	[39]
Ni <sub>2</sub> Cl <sub>2</sub> (BTDD)	1752	-	2.2	0.77	0.3-0.32	-	[39]
Ni-BPP	2039	0.88	1.7	0.72	0.08-0.32	-	[33]
Ni-TPP	1975	1.14	2.3	0.84	0.26-0.64	-	[33]
Ni-IRMOF74- III	-	-	-	0.35	0-0.05	<65°C,	[82]

NU-1500(Cr)	3580	1.28	1.4	1.09	0.45-0.49	25°C, RH<20%	[83]
PIZOF-2(Zr)	1250	0.68	2.0	0.68	0.7-0.74	-	[37, 84]
SIM-1(Zn)	570	0.3	0.65	0.14	-	-	[51]
UiO-66(Zr)	1290	0.49	0.74/ 0.84	0.44	0.3-0.35	-	[37]
+NH <sub>2</sub> (Zr)	1328	0.7	0.75/ 1.2	0.38	0-0.3	-	[80]
Y-shp-MOF-5	1550	0.63	1.2	0.45	0.55-0.72	25°C, RH<45%	[21]
ZJNU-30(Zr)	3116	1.24	0.7/1.4/ 2.1	1.2	0.21	<60°C	[81]

202

### 203 3. Mechanisms and selection criteria of MOFs to the application in the built environment

204 Considering the operational performance of traditional desiccants, solid desiccant technology  
205 suffers from the bulky systems and low efficiency, thus, leading to limited applications [11].  
206 Some efforts have also been made to mix the inorganic salt with desiccants (i.e. silica gel) to  
207 improve the working capacity. However, the regeneration condition is closely related to the  
208 nature of the desiccants, not to ignore the corrosion hazard of the inorganic salts on the metal  
209 framework. It is expected that the novel desiccants could well overcome these drawbacks. In  
210 the following section, the detailed information about the promising MOF-based desiccants has  
211 been presented. The adsorption mechanisms are also noted to disclose the moisture transfer  
212 within the MOF desiccants (Section 3.1). Based on their properties, the selection criteria of  
213 available MOFs have been discussed to further elucidate the advantages of MOF desiccants in  
214 practice (Section 3.2).

215

#### 216 3.1. Water adsorption mechanisms in MOFs

217 Owing to the remarkable features of MOFs, the water adsorption mechanism has drawn  
218 significant research attention, which can be divided into three subgroups: I) chemisorption in  
219 metallic clusters, II) reversible physisorption in layers or cluster adsorption, and III)  
220 irreversible capillary condensation.

221

222 **Chemisorption in metallic clusters:** Due to the accumulation of charges, the unsaturated  
223 metal sites in MOFs evolve into strong adsorption nodes [85]. These strong adsorption nodes  
224 can form initial adsorption sites, followed closely by the weaker nodes. However, to regenerate  
225 MOFs to their full adsorption capacity, extensive extent of thermal energy is needed, which is  
226 undesirable for sorption-based applications. Besides, some studies have reported that the  
227 repeated adsorption/desorption of vapor molecules on these sites may lead to gradual  
228 degradation [56, 86].

229

230 **Physisorption in layers or cluster adsorption:** Surface water molecules initially gather at the  
231 hydrophilic surface sites (i.e. hydroxyl), followed by the adsorbed water molecules acting as  
232 nucleation sites to grow into large water clusters (nucleation growth process). As these clusters  
233 connect with each other through the surface or pores (pore filling process), the continuous  
234 moisture transfer is observed to occur [87]. This mechanism is similar to other conventional  
235 materials like activated carbon, and observed in some MOFs as well.

236

237 **Capillary condensation:** As some porous materials have a hysteretic capillary condensation  
238 phenomenon, the definition of critical diameter indicates that the capillary condensation in  
239 desiccants with certain pore size is generally accompanied by a hysteresis loop in the isotherms  
240 [51]. In contrast to pore filling, it should be noted that the capillary condensation is an

241 irreversible process. As for MOFs with pore size  $<2\text{nm}$ , the presence of hysteresis is generally  
242 assigned to the deformation of inner frameworks [88].

243

### 244 3.2. Selection criteria for MOF desiccants

245 MOFs with special intrinsic properties and adsorption mechanisms have been identified in the  
246 previous sections. Here, the selection criteria were discussed in detail to further elucidate the  
247 assessment of MOFs. To do so, some criteria related to material properties have been presented,  
248 namely stability, performance and safety. Other factor such as scalability belongs to the  
249 manufacturing technologies depend on the improvement of industrial level.

250

#### 251 3.2.1. Stability

252 In many cases, the employment of MOF materials is held back due to the weak long-term  
253 stability. In built environment, the MOF material may quickly break down after moisture  
254 exposure, thus, it is preferable to identify the promising candidates based on the stability studies  
255 reported in literature. Previously, the stability of MOFs upon exposure to water in vapor and  
256 liquid phase has been reviewed in ref. [14], based on which the relationship between the  
257 structure and stability has also been discussed with respect to metal-ligand bonds and  
258 degradation mechanisms (including ligand displacement and hydrolysis) [29, 89-96]. Moreover,  
259 a comprehensive review of heat pumps using MOF desiccants is also available [16]. Burtch et  
260 al. have expediently identified MOF water stability in the thermodynamic and kinetic regimes,  
261 as shown in Fig. 1 [17]. However, the balance between thermodynamic and kinetic control over  
262 MOF water stability remains under debate [97].

263

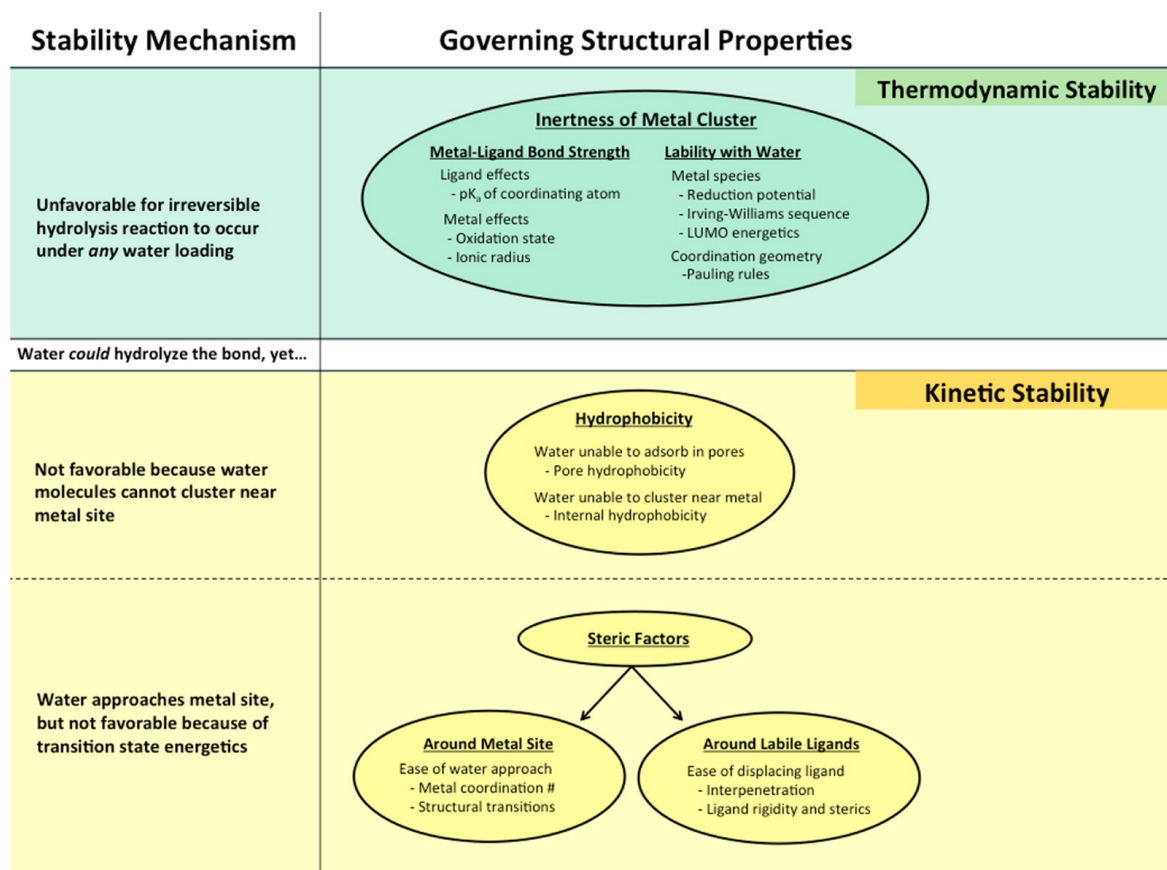


Fig. 1. Structural factors affecting MOF water stability [17].

264

265

266

267 Thermodynamic stability relates the free energy in a hydrolysis reaction to the structural  
 268 properties of MOFs. In other words, the inert degree of the metal cluster directs the  
 269 coordination with water, followed by the destruction of the crystal structure. It is believed that  
 270 a thermodynamically stable MOF can maintain the framework avoiding breakdown after a  
 271 long-time exposure to moisture, and it is concluded to contribute to the strength of metal-ligand  
 272 bond [89, 95, 98] and the lability with water [92, 99]. Under a built environment, the thermal  
 273 stability of MOF materials during moisture transfer still requires further exploitation.

274

275 Kinetic stability is dependent on the activation energy barrier related to the specific reaction.  
 276 Even if a structure may not be thermodynamically stable, high activation energy can still  
 277 restrict the hydrolysis reaction and keep the structure stable in the presence of water. Here, the

278 kinetic stability represents the material resistance to water in the vapor phase [100]. In addition,  
279 some MOFs have been reported to effectively perform in humid air without any degradation,  
280 though breakdown is observed after exposure to liquid water [101]. These MOFs still exhibit  
281 strong potential of use in humid air [38, 78, 102].

282

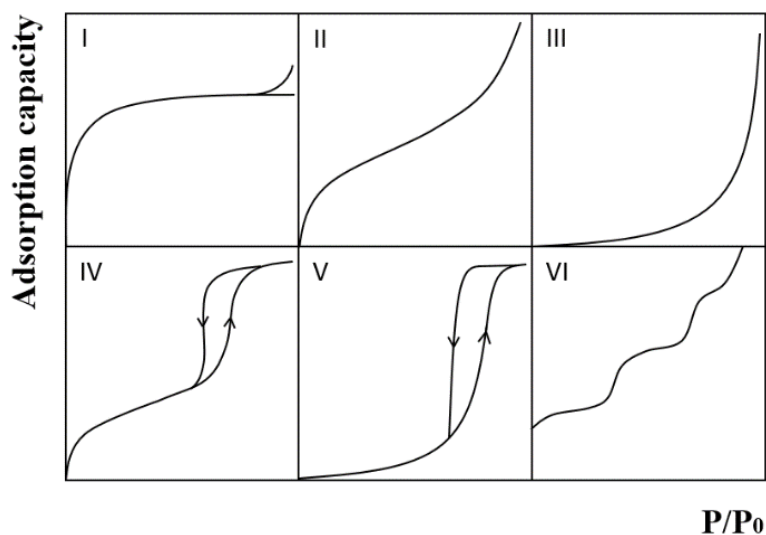
### 283 3.2.2. Performance

284 With respect to the assessment of a practical system, it is inevitable to mention the water  
285 capacity, regeneration condition and sorption dynamics of the desiccant employed. Some  
286 research studies have indicated that a regeneration temperature less than 80°C can lead to  
287 significant improvement in the system performance [20]. High water capacity and dynamic  
288 sorption instead can reduce the time spent in the periodic cycles or system volume.  
289 Consequently, it is desirable to select MOFs with high water capacity and dynamic sorption,  
290 along with gentle regeneration condition.

291

292 Isotherm is a vital tool for characterizing the water capacity and affinity to water vapor for the  
293 desiccant materials [51]. It is known that the water capacity and affinity to water vapor can  
294 affect the adsorption and desorption process. High affinity between the water vapor and  
295 desiccants indicates the difficulty for the adsorbed water molecules to break away from the  
296 formed chemical bonds, thus, signifying a strict regeneration condition. In Fig.2, IUPAC  
297 (International Union of Pure and Applied Chemistry) has classified isotherms for  
298 thermodynamic analysis [103]. However, only desiccants (e.g. MOFs) with type V isotherm  
299 (sigmoidal or S-shaped curve, which enables a sharp change within a narrow  $P/P_0$ ) are the  
300 optimal candidates for sorption-based systems [11]. A sharp increase in adsorption capacity at  
301 low RH is the characteristic of highly hydrophilic desiccants, as presented in Type I, II, IV and  
302 step-like Type VI isotherms. These desiccants (e.g. zeolite (I) and silica gel (II)) generally

303 require more energy to drive the regeneration process. Type III isotherm belongs to the  
304 hydrophobic group, which is not suitable for the system operation due to the higher trigger  
305 point ( $P/P_0$ ). Thus, the selection criteria should at least meet  $>0.2g_{H_2O} g^{-1}$  water capacity and  
306  $<90^\circ C$  regeneration condition.



307

308 **Fig. 2.** Classification of isotherms based on IUPAC (International Union of Pure and  
309 Applied Chemistry) [103].

310

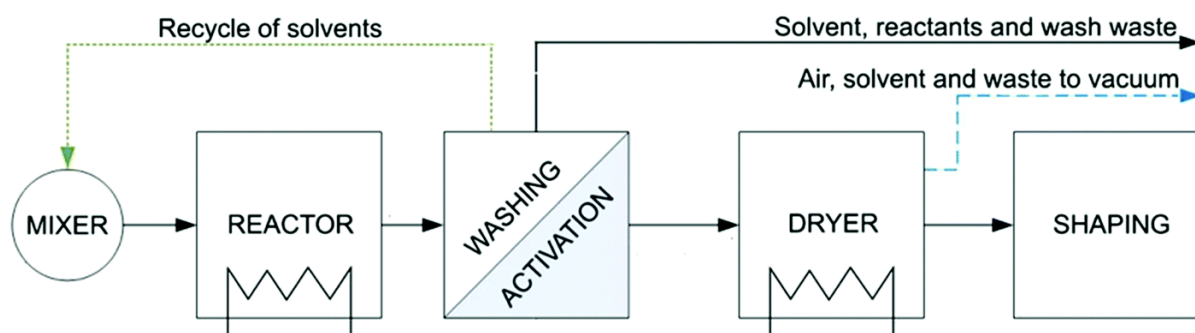
311 With respect to dynamic sorption that indicates the adsorption and desorption equilibrium in  
312 cycles, Thomas et al. initially investigated the adsorption performance of traditional desiccants  
313 [104]. Afterwards, many research studies have reported experimental analysis on activated  
314 carbon and silica gel [105, 106]. Recently, the dynamic nature of the MOF materials has been  
315 evaluated by means of *in-situ* EDXRD [58], thermogravimetric analysis [107], etc. Solovyeva  
316 et al. have reported the high potential of MOF-801 in adsorption cooling through water  
317 adsorption dynamics [73]. In this regard, the dynamic nature of MOFs correlated to material  
318 properties of heat and mass transfer can help to anticipate the future applications [64, 72, 108,  
319 109].



320

### 321 3.2.3. Scalability

322 The translation of novel materials into practical technologies faces the challenge to produce  
323 MOFs at the required scale and quality. For the built environment, an open SDS generally  
324 requires MOFs at the kilogram or ton scale to regulate the latent load, which is quite different  
325 from the gram-scale production of MOFs in laboratory. Recently, factors affecting the scale-up  
326 methods have been comprehensively reviewed, and two aspects can be concluded [110]:  
327 synthesis process and raw materials. Normally, a complete synthesis process includes synthesis  
328 and post-synthesis. The development in the chemical synthesis methods of MOFs have been  
329 discussed for the past 20 years (See Fig. S1, Supporting Information). It is desirable that the  
330 emerging methods are capable to significantly reduce the time spent in the chemical reactions  
331 [111]. After synthesis, careful processing is required in order to qualify the materials, as shown  
332 in Fig.3. Here, processes such as washing and activation lead to the extension of the cycle time.  
333 Thus, meaningful studies on shorting the post-synthesis processes are needed. On the other  
334 hand, raw materials correspond to the possibility of large-scale preparation of MOFs. It is  
335 encouraged to use cost-effective and environmentally friendly raw materials to obtain the  
336 functional MOF materials. To date, large-scale production of some MOF materials has been  
337 reported [6, 16, 44,112,113].



338

339

**Fig. 3.** Basic processes for MOF production [110].

#### 340 3.2.4. Safety

341 Toxicity of MOFs is one of the most important concerns, as these materials may be harmful to  
342 human health on direct contact. The selection of green materials should be of high priority for  
343 specific applications. Thus, among the raw materials for MOF synthesis, the use of  
344 environmentally unfriendly ingredients should be reduced or avoided. Green transition metals  
345 such as Al, Fe, Zr and Cu have been widely recognized as alternatives to Cr-based MOFs due  
346 to the low toxicity and cost [35, 114-116]. Green solvents are also employed during MOF  
347 synthesis. Some of the accepted green solvents such as water, ethanol, ethyl acetate, etc., are  
348 highly recommended, and less green solvents including formic acid, dimethyl sulfoxide,  
349 dimethyl formamide, etc., should be used in moderation [32, 35]. In short, natural or biomass-  
350 based products are good candidates to generate ideal MOFs using low-toxicity metal clusters.  
351 Besides, it is noteworthy that other safety hazards such as inflammability and bacteriostatic  
352 activity all have certain effects on the quality of the built environment.

353

#### 354 **4. Material-level water vapor capture of MOFs**

355 As many MOFs have desired water uptake and regeneration condition, care is necessary to  
356 screen the MOFs suitable for the specific use under specified conditions. Many literature  
357 studies have reported the MOF materials for water harvesting in water scarcity regions and heat  
358 transformation in heat pumps [23, 27, 32, 81, 117]. As an open SDS employed for humidity  
359 regulation of the built environment, it is noteworthy that different MOFs may correspond to  
360 different trigger points, corresponding to different climate conditions. Based on the  
361 classification of the trigger point, MOFs with the following features are focused in this section  
362 (*material level*): 1) high water uptake (more than 0.2 g g<sup>-1</sup>) and stability, 2) gentle regeneration  
363 condition, and 3) steep rise in water uptake.

364

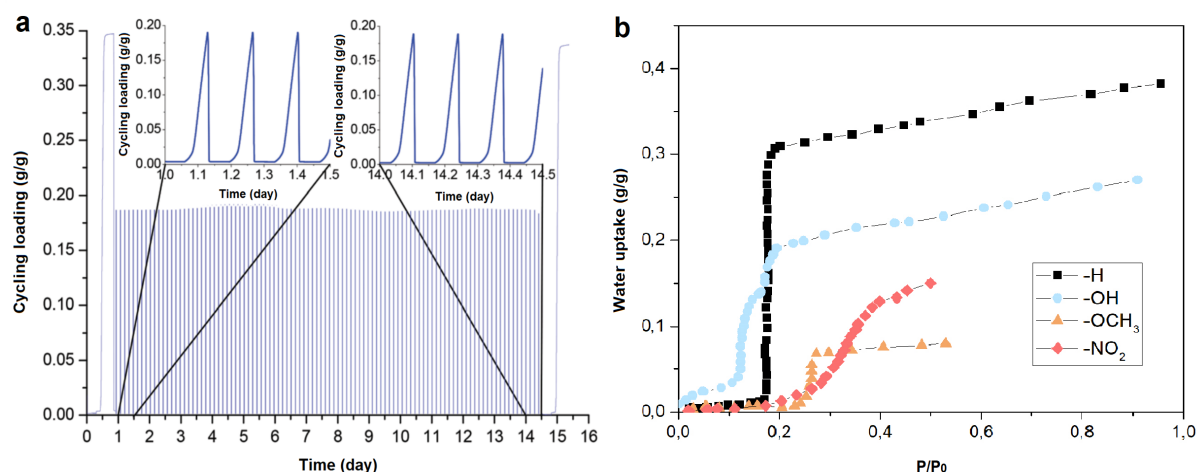
#### 365 4.1. Low range (<30% RH)

366 Desiccants with high water uptake at the low relative pressure have strong affinity towards  
367 water molecules, generally requiring strict regeneration conditions. In comparison with the  
368 traditional desiccants such as silica gel, zeolites, etc., many MOF materials with low trigger  
369 point can still have a low regeneration temperature and high water uptake. With these properties,  
370 active SDS can significantly improve the system performance, while passive SDS can maintain  
371 the low RH level, which is a requirement in some special installations. The humidity control  
372 can effectively avoid, for example, ageing of the batteries in battery factories and deterioration  
373 of artefacts in museums [118]. Thus, the search for MOFs with low trigger point  $P/P_0$  in  
374 isotherms deserves more intensive efforts.

375

376 CAU-10 (CAU: Christian Albrechts University) is a kind of porous aluminum isophthalate,  
377 which combines aluminum clusters with BDC (1,3-benzene dicarboxylic acid) ligand. As a  
378 commercially available MOF, the synthesis method has been greatly improved by substituting  
379 toxic DMF-water solvent (dimethylformamide) with green options [32]. In the framework of  
380 CAU-10, corner-sharing  $AlO_6$  polyhedra are connected with each other, forming a helical  
381 arrangement and square channels with up to 0.7nm pore diameter [19, 38]. Fröhlich et al. [119]  
382 were the first to investigate the hydrothermal stability through 700 adsorption-desorption  
383 cycles with no observed irreversible degradation, as shown in Fig.4 (a). A  $0.34 \text{ g g}^{-1}$  of water  
384 uptake at thermodynamic equilibrium has been observed, accompanied by 0.18  $P/P_0$  trigger  
385 point in the isotherm. CAU-10 coated adsorption chillers [32] have been subsequently prepared,  
386 which indicates that a regeneration temperature of  $70^\circ\text{C}$  can generate a specific cooling power  
387 over  $1200\text{W kg}_{\text{ads}}^{-1}$ . Additionally, several functional groups in the ligands have also been

388 investigated, such as CAU-10(-OH, -OCH<sub>3</sub>, -NO<sub>2</sub>). Reference [38] presents different shapes of  
389 isotherms with even less water uptake at adsorption equilibrium, as shown in Fig.4 (b),  
390 probably resulting from the change in pore volume and heterogeneous character.



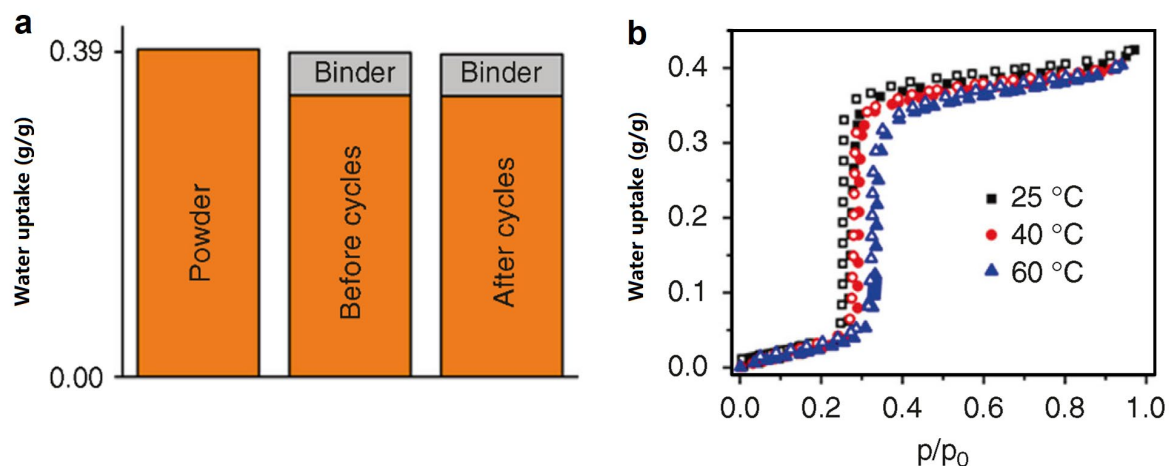
391

392 **Fig. 4.** (a) Cycling performance of CAU-10 [119] and (b) water adsorption isotherms with  
393 different functional groups (25°C) [38].

394

395 CAU-23 is a new class of Al-based MOF with TDC (thiophene-2, 5-dicarboxylic acid) as its  
396 ligand. A recent study has indicated that CAU-23 can be synthesized using a green and scalable  
397 method by using water as the only solvent, and it is stable in air up to 400°C, thus, exhibiting  
398 high thermal stability [20]. In the three-dimensional structure of CAU-23, the metal cluster unit  
399 comprises of the combination of helix and straight AlO<sub>6</sub> polyhedra, joined with TDC to form  
400 square channels. CAU-23 has been tested for 5000 cycles with nearly no loss in water uptake  
401 as shown in Fig.5 (a). Water isotherm indicates that a maximum water uptake of 0.43g g<sup>-1</sup> can  
402 be obtained without hysteresis loop at room temperature. Correspondingly, the trigger point is  
403 noted to be around 0.24 P/P<sub>0</sub>. Besides, the findings from the desorption analysis have pointed  
404 out an ultralow regeneration temperature of <60°C for the adsorption-driven chillers, along  
405 with a cycling water capacity of 0.37g g<sup>-1</sup> [20]. As the temperature increases, the trigger point

406 of the isotherms in Fig.5 (b) is observed to move right to a larger  $P/P_0$  with lower water capacity.  
407 Other analogues of CAU-23 such as CAU-22 [120], CAU-28 [121] and CAU-39 [122] are  
408 more or less limited by the low hydrothermal stability or low uptake capacity.



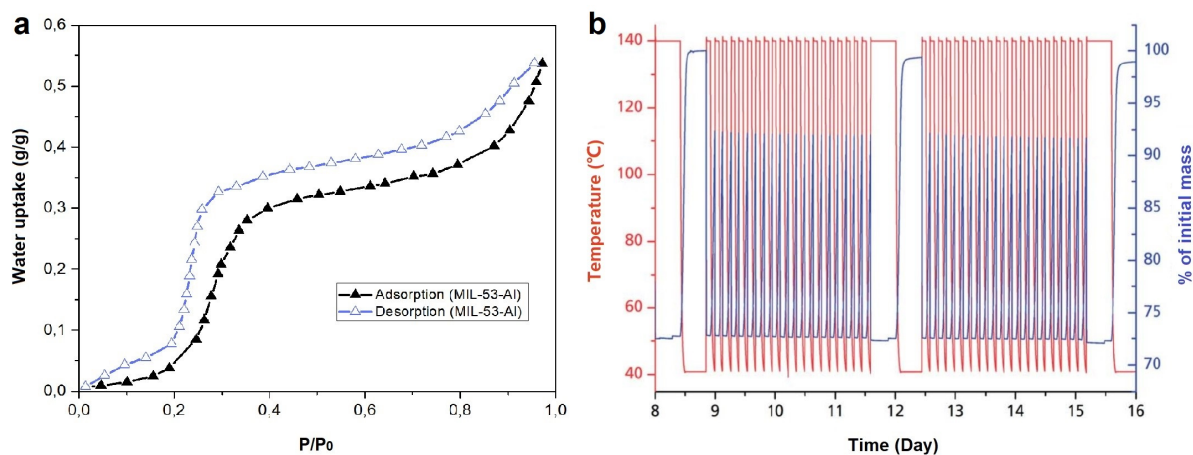
409

410 **Fig. 5.** (a) Water uptake of CAU-23 coatings before and after 5000 cycles and (b) water  
411 adsorption/desorption isotherms of CAU-23 at different temperatures [20].

412

413 MIL-53 (Al, Fe, Cr) [MIL: Material Institut Lavoisier] is one of the most frequently  
414 investigated MOF series. Among the various analogs, MIL-53 (Al) is currently produced at  
415 industrial levels and features corner-sharing  $AlO_6$  chains connected by terephthalate ligands in  
416 the crystal structure. To date, MIL-53(Al) has been prepared at large scale by sole use of water  
417 as solvent, however, the recorded water capacity is far less than  $0.2 \text{ g g}^{-1}$  [123]. Subsequently,  
418 Alvarez et al. have investigated a new MOF [114], MIL-53-FA (or aluminum fumarate), which  
419 has an isoreticular structure to MIL-53(Al). Although these have similar corner-sharing  
420 aluminum-based octahedra, MIL-53-FA uses fumarate as its ligands. As a commercially  
421 available product with green synthesis, MIL-53-FA has been widely applied for gas storage and  
422 water vapor capture [71]. Henninger et al. [18, 52] also reported the highly stable nature of the  
423 hydrophilic MIL-53-FA. As shown in Fig. 6, the cycling adsorption capacity is observed to be

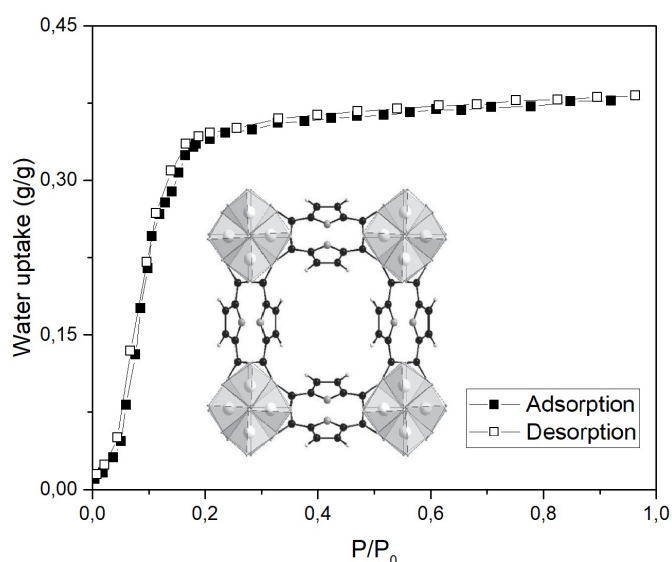
424 constant at around  $0.37\text{ g g}^{-1}$  after 4500 cycles. The isotherm shows a steep rise in water uptake  
 425 between 0.2-0.35  $P/P_0$ . Regeneration at  $90^\circ\text{C}$  achieved the release of more than half of the  
 426 adsorbed water molecules within several minutes, which is superior to the zeolites ( $>100^\circ\text{C}$ ).



427  
 428 **Fig.6.** Water adsorption/desorption isotherms of MIL-53-FA at  $25^\circ\text{C}$  [48] and cycling tests  
 429 [52].

430  
 431 Serre et al. reported hydrophilic MOF (MIL-160), a promising material for heat reallocation,  
 432 which consisted of aluminum ions and FDCA (2, 5-furandicarboxylic acid, derived from  
 433 renewable biomass feedstock) ligand [25]. As an isostructure to CAU-10, hydrothermally  
 434 stable MIL-160 has helically cis-connected chains with four surrounding carboxylates forming  
 435 square-shaped channels as shown in Fig. 7. The subsequent studies indicated that MIL-160  
 436 with 0.5nm pore size outperforms CAU-10 in surface area and pore volume [25]. Though the  
 437 water uptake of MIL-160 is almost identical to CAU-10, its 0.05  $P/P_0$  trigger point exhibits  
 438 better hydrophilicity than 0.16  $P/P_0$  for CAU-10 due to the presence of many hydroxyl groups  
 439 at the pore surface. The measured water uptake is around  $0.37\text{ g g}^{-1}$ , and most of the water  
 440 adsorption is below 0.18  $P/P_0$ . The high water affinity enables a heat source around 363K  
 441 ( $90^\circ\text{C}$ ) to achieve the release of 75% of the water molecules (regeneration). Lately, the authors

442 have also investigated the energy-storage capacity and cycling loading lift of MIL-160, which  
443 are noted to be 6 times as compared to zeolite 13X [124]. Based on these features, MIL-160 is  
444 a promising desiccant for adsorption heat transformation (i.e. heat pump) [125] and even in  
445 places requiring an ultralow relative humidity with gentle regeneration condition.



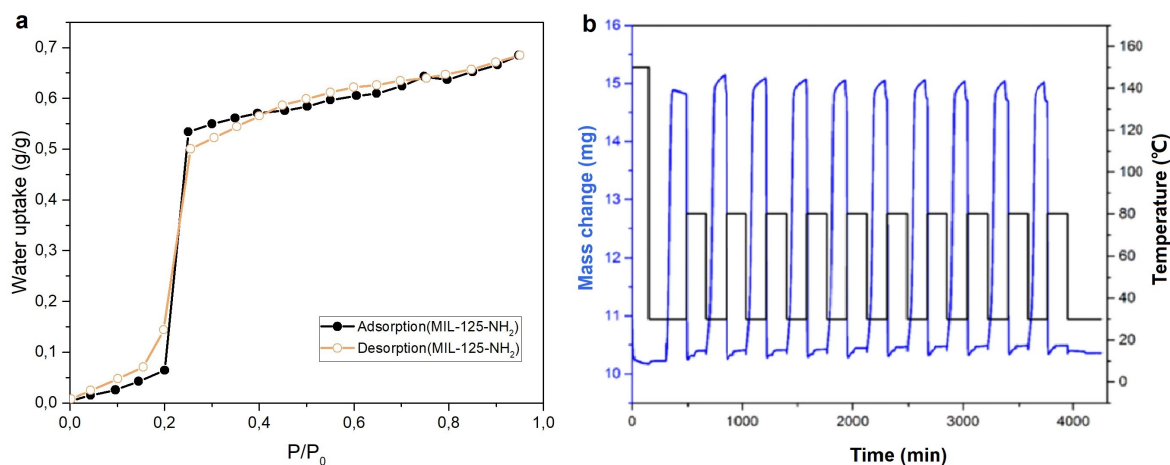
446

447 **Fig. 7.** Water adsorption/desorption isotherms for MIL-160 [25].

448

449 MIL-125-NH<sub>2</sub> is a Ti-based MOF comprised of titanium clusters and BDC-NH<sub>2</sub> (2-amino  
450 benzene dicarboxylic acid) with two types of cages (0.51nm and 1.25nm). Since Dan-Hardi et  
451 al. [126] reported the synthesis of highly porous MIL-125, the ligand functionalization has been  
452 applied to generate MIL-125-NH<sub>2</sub> [127, 128]. MIL-125-NH<sub>2</sub> has a three-dimensional  
453 bipyramidal structure with Ti<sub>8</sub>O<sub>8</sub>(OH)<sub>4</sub> as metal node connected with eight BDC-NH<sub>2</sub> ligands.  
454 It is reasonable to expect a reduction in pore size and surface area owing to the introduction of  
455 the amino group, but isotherms exhibit an obvious increase in the water uptake for MIL-125-  
456 NH<sub>2</sub> compared to unusual adsorption and desorption behavior of MIL-125. This indicates that  
457 MIL-125-NH<sub>2</sub> is more hydrothermally stable in presence of water [129]. A recorded 0.67 g g<sup>-1</sup>  
458 water uptake with 0.2 P/P<sub>0</sub> trigger point in Fig.8 confirm the competence of MIL-125-NH<sub>2</sub> for

459 hygrothermal control at low RH range. Kim et al. have investigated its potential use in the  
 460 adsorption heat transformation, and regeneration at 80°C with a constant cycling water  
 461 capacity of 0.45 g g<sup>-1</sup> at working conditions confirm its superiority as compared to most of the  
 462 currently used desiccants [48].

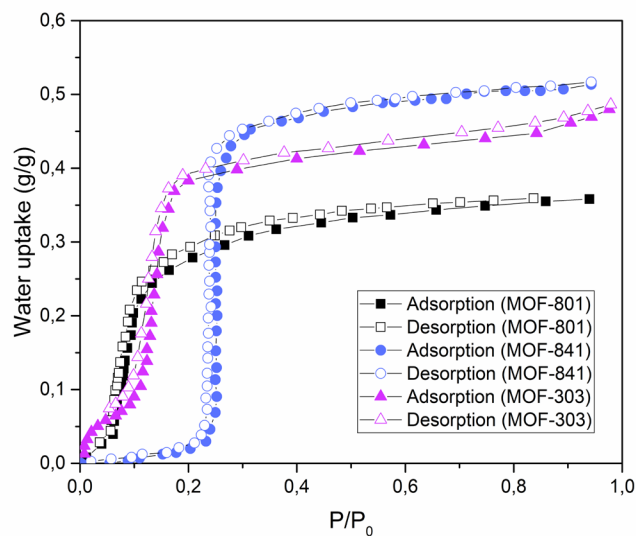


463  
 464 **Fig. 8.** (a) Water adsorption/desorption isotherms for MIL-125-NH<sub>2</sub> and (b) dynamic water  
 465 uptake with adsorption at 30°C and desorption at 80°C [48].

466  
 467 In recent years, MOF-801 has attracted research attraction for use in applications requiring low  
 468 RH range, such as water harvesting in deserts. Behrens et al. [36] first reported the preparation  
 469 of MOF-801 by combining a zirconium cluster (Zr<sup>4+</sup>) with fumaric acid. The structure of MOF-  
 470 801 is composed of cubic spaces with three independent cavities, two tetrahedral cavities of  
 471 size 0.56nm and 0.48nm, and one octahedral cavity with a diameter of 0.74nm. MOF-801 has  
 472 been demonstrated to be stable in hygrothermal conditions, and its cycling water uptake  
 473 remains stable after five adsorption-desorption cycles [37]. The adsorption isotherm in Fig.10  
 474 displays a steep rise around trigger point (P/P<sub>0</sub>) of 0.05 and reaches a saturated state around 0.5,  
 475 from which a water uptake capacity of 0.36g g<sup>-1</sup> at room temperature can be observed, greatly  
 476 outperforming the traditional desiccants (i.e. silica gel). Subsequently, Yaghi et al. have



477 prepared MOF-841 and other analogs such as MOF-802, MOF-805, MOF-806 and MOF-808,  
478 however, the latter ones demonstrate unstable water adsorption during initial cycles owing to  
479 the loss of porosity [37]. MOF-841 is prepared by employing MTB (4,4',4'',4'''-  
480 methanetetrayltetrabenzoic acid) as connecting ligand. In the three-dimensional framework of  
481 MOF-841, the metal cluster bound with eight ligands constructs the basic structural unit.  
482 Cycling performance indicated that MOF-841 exhibits relatively constant adsorption after  
483 several cycles. Its steep rise in Fig.9 occurs around 0.26 P/P<sub>0</sub>, and it reaches saturation around  
484 0.3 P/P<sub>0</sub>, at which the water uptake accounts for nearly 90% of total water uptake (0.5g g<sup>-1</sup>).  
485 Recently, Yaghi et al. [23, 117] applied MOF-801 for water harvesting from air. The  
486 experiments were conducted with a regeneration temperature of 65°C, and the set-up was  
487 predicted to produce a 2.8L<sub>water</sub> kg<sub>MOF</sub><sup>-1</sup> each day at 0.2 P/P<sub>0</sub>. Based on this study, the authors  
488 also developed a next-generation desiccant MOF-303, synthesized by using aluminum-based  
489 metal cluster and HPDC [1H-pyrazole-3,5-dicarboxylate] [22]. The green hydrophilic MOF  
490 featured pore volume and pore size of 0.54cm<sup>3</sup> g<sup>-1</sup> and 0.6nm, with up to 0.48g g<sup>-1</sup> of water  
491 capacity. The trigger point is noted to be around 0.15P/P<sub>0</sub>, which is comparable to its  
492 predecessor MOF-801. In addition, 150 cycling experiments verified the hydrolytic stability of  
493 the material owing to no measurable mass loss. Fig.10 shows the evolution and cycling  
494 performance of the crystal structure from MOF-801 to MOF-303. MOF-303 with higher  
495 cycling water lift is theoretically superior to MOF-801 for humidity regulation.

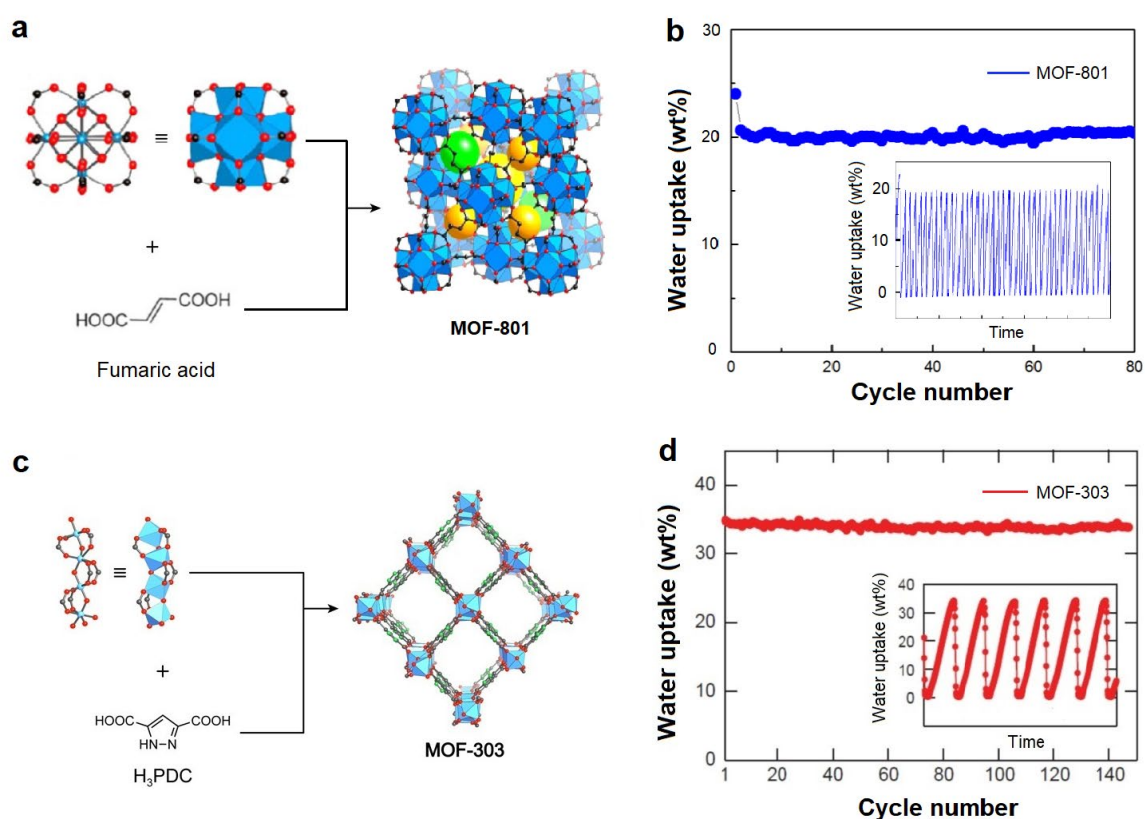


496

497 **Fig. 9.** Water adsorption/desorption isotherms of different MOFs used for water harvesting

498

[22, 37].



499

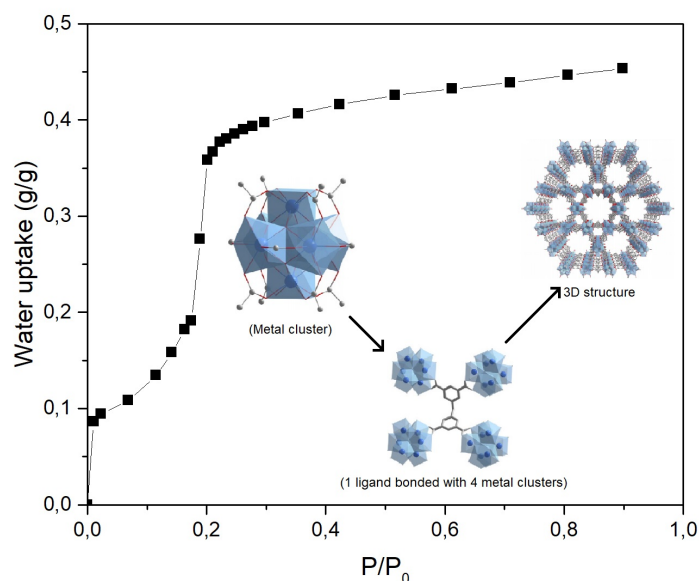
500 **Fig.10.** Crystal structure (a and c) and cycling performance (b and d) of MOF-801 and MOF-

501

303 [22, 37].

502

503 MIP-200 is a newly developed MOF material constructed using the zirconium cluster and  
504 H<sub>4</sub>mdip ligand (3, 3', 5, 5'-tetracarboxydiphenylmethane). In the three-dimensional structure,  
505 Zr-based metal cluster is connected with eight carboxylate groups and four formate groups,  
506 thus, forming a triangular tunnel of 0.68nm and a hexagonal channel of 1.3nm. A surface area  
507 of 1000m<sup>2</sup> g<sup>-1</sup> as well as a pore volume of 0.4cm<sup>3</sup> g<sup>-1</sup> were measured as well. Serre et al. [46]  
508 explored the application of MIP-200 in adsorption-based chillers. From isotherm in Fig. 11,  
509 MIP-200 is noted to exhibit high water capacity of around 0.46 g g<sup>-1</sup>, however, a two step rise  
510 occurred at 0.01P/P<sub>0</sub> and 0.17 P/P<sub>0</sub>, respectively. It is also found that the material is stable  
511 against different chemicals and temperatures over 300°C. One intriguing property is the facile  
512 regeneration temperature below 70°C, which outperforms most of currently reported desiccants,  
513 such as MIL-160 (90°C), SAPO-34(~90°C), aluminum fumarate (90°C), etc. [20]. Other family  
514 members such as MIP-202, MIP-203 and MIP-204 have also been synthesized. However, the  
515 ultra-small porosity limits their application [130].



516

517

**Fig. 11.** Water sorption isotherms of MIP-200 at 25°C [20, 46].

518

519 The MOFs described so far represent both widely used desiccants as well as newly developed  
520 desiccants. These desiccants feature low trigger point (0-30%), exhibiting great potential of  
521 application for the control in built environment. In addition, other promising desiccants such  
522 as  $M_2Cl_2(BTDD)$  ( $M=Co, Ni$ ) [26, 39], mixed-metal MOF [10], ZJNU-30 [81], CUK-1[30],  
523 etc., demonstrate strong capability for humidity control. The exploitation of these MOFs is still  
524 an ongoing research.

525

#### 526 4.2. Medium range (30~65% RH)

527 In the past few years, a few MOFs have been reported with a medium trigger point. Though  
528 these MOFs may have weak affinity towards water molecules, the water capacity and  
529 regeneration condition are still significant. Hydrophilic MOFs might be preferred for the active  
530 systems due to high working efficiency. However, a few studies carried out by using these  
531 neutral MOFs have also indicated that these desiccants are well capable of sorption-based heat  
532 transformation [27]. On the other hand, as ASHRAE has recommended the comfort zone of  
533 relative humidity,  $>65\%RH$  and  $<30\%RH$  to a degree make human beings to feel  
534 uncomfortable. Materials that can adsorb water vapor at higher humidity levels and desorb it  
535 at lower humidity levels can well meet the demand for humidity control in a passive way.  
536 Traditional materials have limited performance in both active and passive SDS. Many research  
537 studies have focused on exploring neutral desiccants and most of these deserve further study.

538

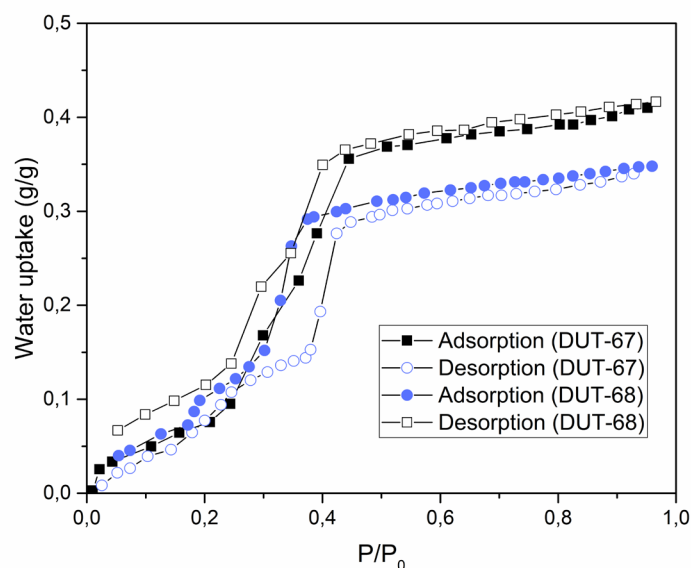
539 CAU-1 was first synthesized by the combination of  $H_2N-H_2bdc$  (aminoterephthalic acid) and  
540  $Al_8(OH)_4(OCH_3)_8$  (aluminum-based octameric cluster) by Stock et al. [131]. The  $AlO_6$ -based  
541 octameric clusters are connected to other units to form two types of cages, an octahedral cage

542 of 1nm and a tetrahedral cage of 0.5nm. The remarkable water uptake at 25°C is recorded  
543 around 0.55g g<sup>-1</sup> [77, 132], and the TGA data exhibit that the material can keep stable under  
544 hydrothermal conditions and preserve its framework up to 310°C [131]. Subsequently, a new  
545 Al-based MOF named CAU-3 has been synthesized, which exhibits water uptake of up to 0.51  
546 g g<sup>-1</sup>. However, the thermal stability tests indicate that the decomposition of framework may  
547 occur in air under 200°C [133]. Reinsch et al. have reported the green synthesis of CAU-15-  
548 Cit [134]. CAU-15-Cit exhibited a 23.8% water uptake at the trigger point of 0.5P/P<sub>0</sub>, and the  
549 powder X-ray diffraction (PXRD) disclosed the reversible de- and rehydration behaviors,  
550 which greatly outperform the unstable form CAU-15 [135].

551

552 As a member of DUT series (DUT, Dresden University of Technology), DUT-68 has been  
553 synthesized by using TDC (2, 5-thiophenedicarboxylate) as ligand with different metal clusters  
554 (Zr-based and Hf-based). Senkowska et al. [136] reported the structure of DUT-68 to contain a  
555 complicated pore system with four types of pore size (0.8nm, 1.25nm, 1.39nm and 2.77nm).  
556 From water adsorption studies, it is observed that a steep rise in water uptake takes place at  
557 0.38P/P<sub>0</sub> exhibiting a value of 0.29 g g<sup>-1</sup>, along with structural stability verified by using  
558 repeated water adsorption tests. Besides, it is noted to adsorb nearly 40% of total water uptake  
559 at <30% RH, which may result from the complex hierarchical pore system. Recently, an insight  
560 into water adsorption by DUT-67 has been proposed for exploring its potential in adsorption-  
561 based heat transformation. Bon et al. [49] conducted more than 20 adsorption-desorption cycles  
562 to prove its stability and investigated the pore filling process through neutron powder  
563 diffraction. In comparison with the other Zr-based DUT-68, Fig.12 indicates that DUT-67 has  
564 a water capacity of 0.44g g<sup>-1</sup> at 0.6 of P/P<sub>0</sub> with a steep rise in relative pressure range 0.3-0.4.  
565 In this respect, DUT-67 is confirmed to be potential desiccant for water adsorption [31]. Other

566 DUT series such as DUT-52, DUT-53 and DUT-69 have been prepared. Though a few of these  
567 may have S-shaped adsorption isotherms, the shape of desorption branch is significantly  
568 different from Type-V isotherms, thus, these are not suitable for humidity control [49, 136].



569

570 **Fig.12.** Water adsorption/desorption isotherms of water-stable DUT series [49].

571

572 MIL-100 is one of the most studied MOF benchmarks for water adsorption applications. To  
573 date, three metal elements such as Fe, Al and Cr have been mostly used with BTC (1,3,5-  
574 benzene tricarboxylic acid) as ligand to prepare MIL-100 series. Since Férey et al. [137]  
575 reported the three-dimensional (3D) structure of MIL-100(Cr), a corner-sharing tetrahedral  
576 MOF(Cr) with 2.5-3nm and 0.65nm sized mesopores and micropores respectively, many  
577 research studies have reported the stability for water adsorption, along with its application in  
578 sensible and latent load control [40, 138]. Kitagawa et al. [40] conducted more than 2000  
579 adsorption-desorption cycles with no observed structural decomposition, and the water uptake  
580 was maintained at 0.8g g<sup>-1</sup>. However, the undesirable isotherms have also driven the efforts to  
581 graft some hydrophilic groups on the coordinately unsaturated metal sites to tune the isotherm  
582 shape of MIL-100(Cr). The introduction of hydrophilic groups tunes the hydrophilicity of MIL-

583 100(Cr), however, decreases the surface area and pore volume, thus, resulting in different  
584 trigger point ( $P/P_0$ ) as well as water uptake capacity [139].

585

586 In addition, considering the potentially harmful chromium compounds, Horcajada et al. have  
587 successfully synthesized Fe-based MOF, MIL-100(Fe) with non-toxic nature [140].  
588 Subsequently, Henninger et al. [27] have used MIL-100(Al, Fe) for heat transformation  
589 applications. From the comparison of isotherms in Fig.13, the water uptake of  $0.77\text{g g}^{-1}$  for  
590 MIL-100(Fe) is noted to be superior than  $0.5\text{g g}^{-1}$  for MIL-100(Al) with, and all of the studied  
591 MOFs bear hydrothermal cycling stability under 40 cycling experiments (6.4% loss for MIL-  
592 100(Fe) and 6.6% loss for MIL-100(Al)), as shown in Fig.14. From the adsorption behavior, it  
593 is interesting to find two step steep rise at 0.24 and  $0.35P/P_0$  for MIL-100(Fe, Al), respectively,  
594 which is similar to 0.24 and  $0.38P/P_0$  observed for MIL-100(Cr). The observed behavior is  
595 explained as follows: the open metal sites start adsorbing a fraction of water molecules below  
596  $0.2P/P_0$ , and subsequently the two steep rise steps contribute to the sudden adsorption in the  
597 cage of different size [45]. The resulting features therefore render MIL-100 series very  
598 interesting alternatives for sorption-based heat and humidity control.

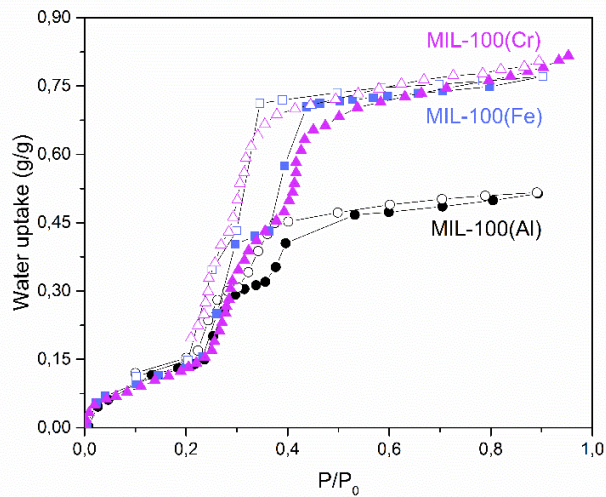


**Fig. 13.** Water adsorption/desorption isotherms of MIL-100 (Al, Cr, Fe) [27, 40, 138].

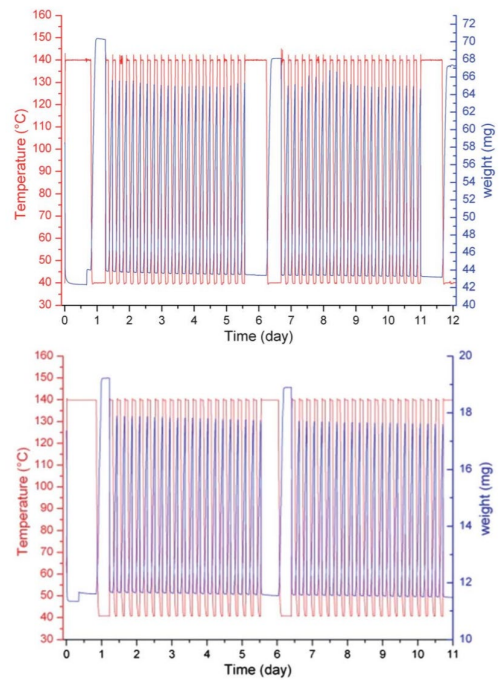


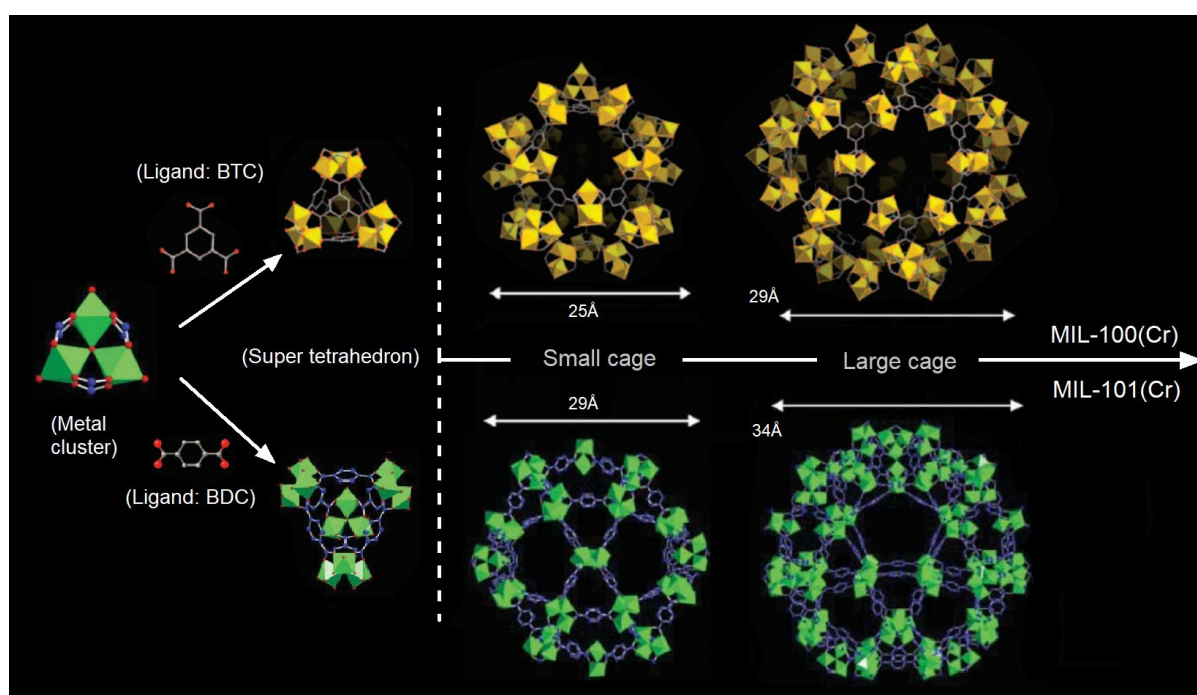
**Fig. 14.** Temperature profiles and mass loading of MIL-100 (Al, Fe) in cyclic tests [27].

599

600 MIL-101 was first prepared and reported by Férey et al. [41] with  $5900 \text{ m}^2 \text{ g}^{-1}$  surface area and  
 601 2.9-3.4nm pore size. The three-dimensional structure is constructed by joining Cr-based  
 602 inorganic trimers (octahedra) with ligand 1, 4-BDC (1, 4-benzenedicarboxylate) to form a super  
 603 tetrahedron, which is closely related to the structure of MIL-100, as seen in Fig.15. With an  
 604 aim to surpass its predecessor's merit of reversible water adsorption, Henninger et al. [29]  
 605 evaluated MIL-101(Cr) and pointed out its more desirable isotherm, with a steep rise at  $0.4P/P_0$ .  
 606 The results indicated nearly  $1 \text{ g g}^{-1}$  of cycling water loading under a typical condition with only  
 607 3.2% of loading loss after 40 cycles on applying MIL-101(Cr) in a heat-transformation cycling  
 608 system. Thus, MIL-101(Cr) is confirmed to demonstrate high water loading along with strong  
 609 hydrothermal stability. Fig.16 shows several isotherms extracted from the literature studies  
 610 indicating ultrahigh adsorption capacity of MIL-101(Cr) with a maximum value reaching up



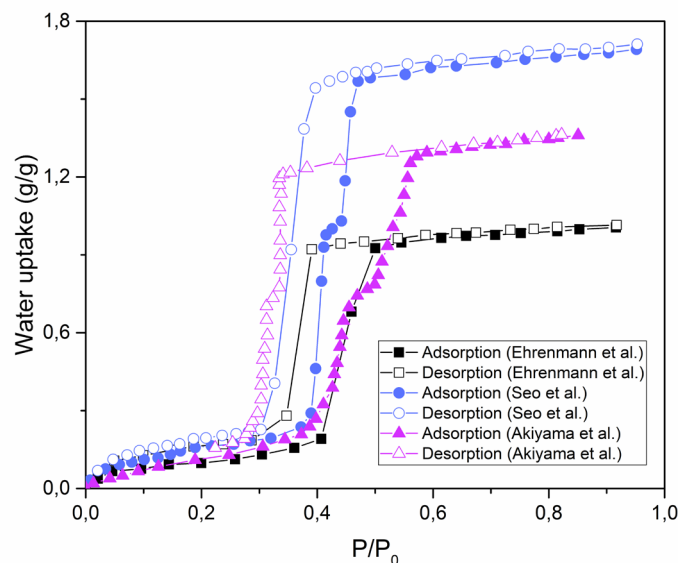
611 to  $1.6\text{g g}^{-1}$  [28, 57, 78]. Owing to the larger pore size ( $>2\text{nm}$ ), hysteresis loops occurred in  
612 isotherms, therefore reducing the usable loading lift in active SDSs. Kitagawa et al. [57] also  
613 examined the adsorption/desorption behavior of functionalized MIL-101 derivatives. These  
614 compounds with different substituents ( $-\text{NO}_2$ ,  $-\text{NH}_2$ ,  $-\text{SO}_3\text{H}$ ) are noted to reach a water capacity  
615 in the range  $0.8\text{-}1.2\text{g g}^{-1}$  with great stability and regeneration under  $80^\circ\text{C}$  [28, 57]. Different  
616 from MIL-100 series, little research has been carried out on MIL-101 analogues with different  
617 metal clusters (i.e.  $\text{Fe}^{3+}$ ,  $\text{Al}^{3+}$ ) due to the hydrolysis.



618

619 **Fig.15.** Structure of MIL-100(Cr) and MIL-101(Cr) [6, 141].

620

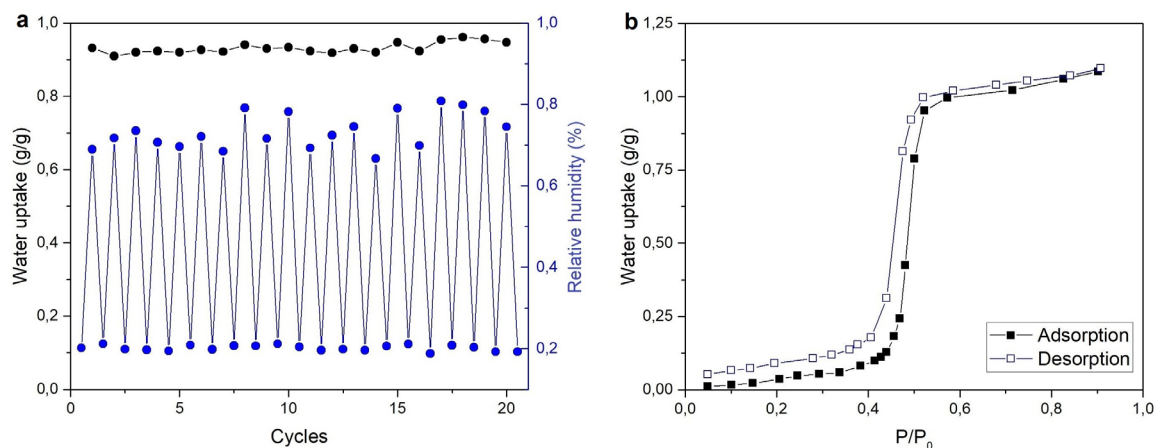


621

622 **Fig. 16.** Water adsorption/desorption isotherms of different MIL-101(Cr) samples [29, 57,  
623 78].

624

625 Many MOFs based on NU series (NU, Northwestern University) have emerged recently,  
626 however, their use for water adsorption has been limited except NU-1500 [142, 143]. Farha et  
627 al. [83] reported that NU-1500 consisted of trivalent trinuclear metal cluster ( $\text{Fe}^{3+}$ ,  $\text{Sc}^{3+}$  and  
628  $\text{Cr}^{3+}$ ) and trigonal prismatic ligand, while the Cr-based NU-1500 was also noted to exhibit  
629 water stability after 20 cycling experiments. In Fig.17(a), water adsorption capacity of NU-  
630 1500 is observed to approach  $1.09\text{ g g}^{-1}$  without hysteresis loop between the adsorption and  
631 desorption branches. This may have resulted due to only one kind of small hexagonal channels  
632 with a 1.4nm of pore size. The trigger point in Fig.17(b) is around  $0.45P/P_0$  followed by a  
633 narrow steep rise. Consequently, compared with more hydrophilic MOFs (low trigger point),  
634 it is reasonable to predict that NU-1500 can be desorbed using a gentler regeneration condition  
635 in heat-transformation application.

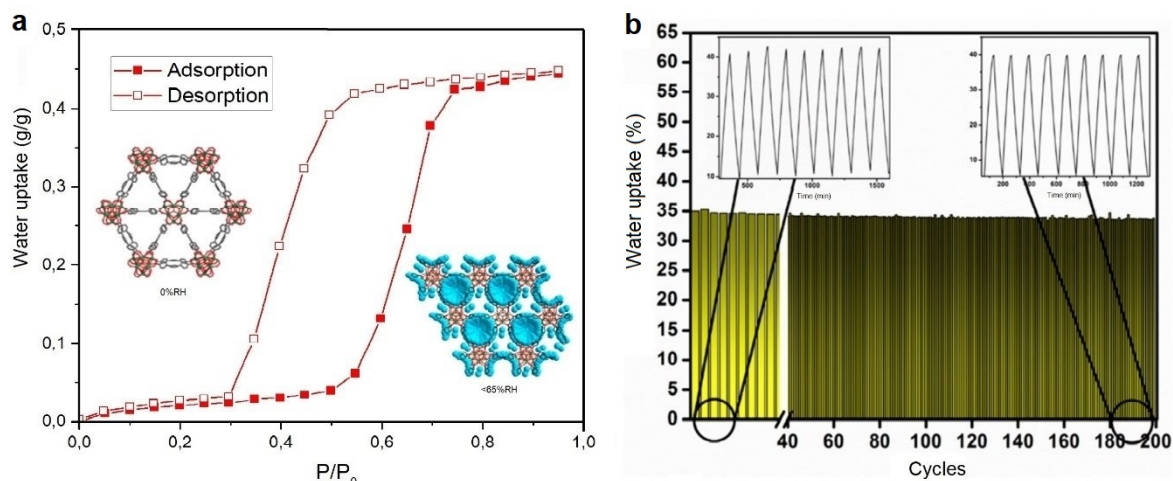


636

637 **Fig.17.** Water adsorption/desorption isotherms and cycling tests between 20%-80%RH [83].

638

639 Recently, two excellent MOFs aimed towards autonomous indoor humidity control have been  
 640 proposed, namely, Y-shp-MOF-5 and Cr-soc-MOF-1. Y-shp-MOF-5 is the rare earth metal-  
 641 based MOF composed of the yttrium-based metal cluster and tetratopic ligand [BTEB, 1,2,4,5-  
 642 tetrakis(4-carboxyphenyl) benzene]. Eddaoudi et al. [21] have evaluated the water  
 643 adsorption/desorption isotherms and cyclic behavior of hexagonal prism-shaped Y-shp-MOF-  
 644 5. The trigger points of adsorption and desorption branches are 0.56 and 0.47P/P<sub>0</sub> respectively,  
 645 as shown in Fig.18(a), after which two steep rise steps occur within 30%-47% RH and 56%-  
 646 70%RH. The water uptake is noted to reach up to 0.45g g<sup>-1</sup>, which indicates superior  
 647 performance as compared to most traditional desiccants. In addition, 200 adsorption-desorption  
 648 cycles display its stable water uptake variation for relative humidity between 25%-85%  
 649 (Fig.18(b)), exhibiting the capacity to regulate the humidity within a desirable range.



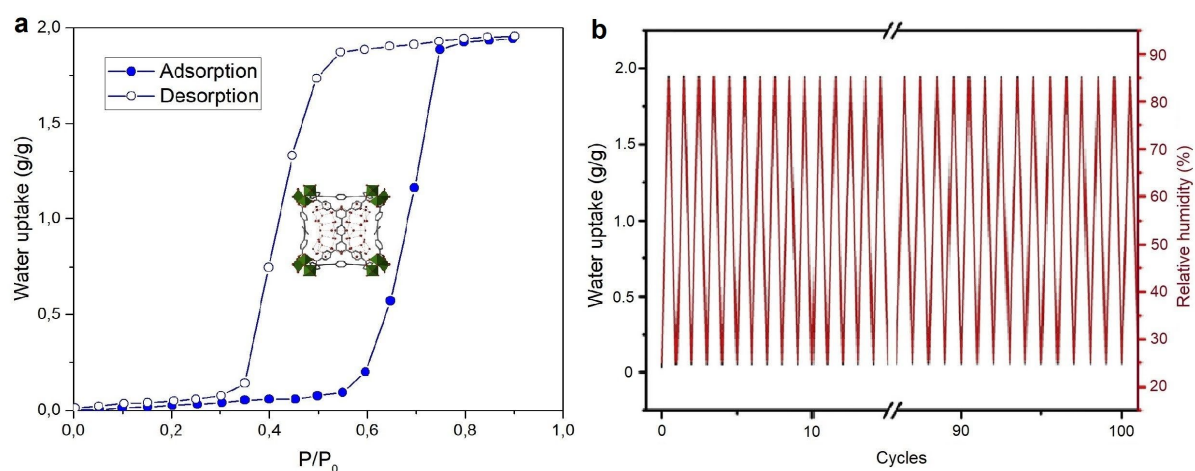
650

651 **Fig.18.** (a) Water adsorption/desorption isotherms of Y-shp-MOF-5 and (b) 200 cycles in the  
 652 relative humidity range between 25% and 85% [21].

653

654 Cr-soc-MOF-1 is the other MOF with potential for autonomous humidity regulation. Eddaoudi  
 655 et al. [42] reported this hydrolytically stable material together with its remarkable water  
 656 capacity ( $\sim 1.95 \text{ g g}^{-1}$ ), much better than the MOFs reported so far. Cr-soc-MOF-1 consists of  
 657 the trinuclear chromium cluster and deprotonated organic ligand (TCPT; 3, 3'', 5, 5''-  
 658 tetrakis(4-carboxyphenyl)-p-terphenyl), developed through post-synthetic modification of Fe-  
 659 soc-MOF-1. The isotherm in Fig.19(a) indicates its intriguing ability for the passive control of  
 660 indoor humidity load in view of the strong hydrolytically stable nature, with 3 times higher  
 661 working capacity ( $1.95 \text{ g g}^{-1}$  at  $0.7P/P_0$ ) than the predecessor, Y-shp-MOF-5, at room  
 662 temperature (298K). The rectangular hysteresis loop with two trigger points in adsorption  
 663 ( $0.6P/P_0$ ) and desorption ( $0.42P/P_0$ ) branches comply with the recommended comfort zone by  
 664 ASHRAE. Besides, the adsorption-desorption cycles were conducted to confirm the durability  
 665 of the material within 25%-85% humidity level at room temperature. After 100 cycling  
 666 experiments as shown in Fig.19(b), the water capacity remained unchanged, which indicated  
 667 that the adsorbed water molecules can be desorbed at 298K by lowering the humidity level.

668 However, the hydrothermal stability at different temperatures is required for active control in  
669 SDSs.



670

671 **Fig.19.** (a) Water adsorption/desorption isotherms of Cr-soc-MOF-1 and (b) 100 cycles in  
672 relative humidity range between 25% and 85% [42].

673

674 On the basis of the previous discussion, the relatively hydrophobic MOFs have less affinity  
675 towards water molecules, thus these theoretically allow swift release of the adsorbed water  
676 molecules. In fact, little research has been carried out to investigate the active heat  
677 transformation owing to the low water uptake at the low relative pressure range. Moreover,  
678 most of these MOFs have an unwanted hysteresis loop, which reduces the actual loading lift.  
679 Luckily, the design and synthesis of these MOFs with hysteresis loop is potentially qualified  
680 for the autonomous humidity regulation in a built environment. The benchmark material Y-  
681 shp-MOF-5 [21] and its successor Cr-soc-MOF-1 [42] have been the most mentioned for the  
682 passive control of indoor humidity load in open SDSs due to their desirable isotherms, high  
683 hydrolytical stability and water uptake. However, these materials have undesirable metal  
684 clusters (i.e. Y, Cr), which may limit their application range. Moreover, further cycling  
685 experiments under different temperature pairs (adsorption-desorption) are needed to be

686 conducted to evaluate their hydrothermal stability for active SDS systems. Besides, other water  
687 stable materials such as MAF [79], DMOF [89], Ni-BPP [33], BUT [76] and functionalized  
688 MOFs [62, 144] have been developed, all of which need further intensive studies for passive  
689 and active humidity control.

690

#### 691 4.3. High range (>65%RH)

692 Some MOF materials with the adsorption process starting after 0.65 P/P<sub>0</sub> trigger point have  
693 also been synthesized. Compared to the earlier-mentioned MOFs, these ultra-hydrophobic  
694 MOFs are less competitive towards the sorption-based humidity regulation due to their low  
695 efficiency for passive (adsorption at >65%RH) and active control (<30%RH) in SDSs. To date,  
696 it is reported that PIZOF-2 [23, 37] initiates water vapor adsorption after 0.7P/P<sub>0</sub> and reaches  
697 68wt% of water capacity at 0.9P/P<sub>0</sub>. Kitagawa et al. [123] investigated MIL-53 (Al) with  
698 different functional groups, and isotherms show a steep rise of water uptake after 0.7P/P<sub>0</sub> in  
699 MIL-53(Al)-OH. Though these MOFs exhibit more or less good stability and S-shaped  
700 isotherms with high water uptake, the hydrophobicity makes them ineffective to take up the  
701 water vapor molecules at the desirable humidity range. It is expected that modification/  
702 functionalization of these MOFs can tune their inner structure, enabling them to exhibit  
703 improved performance based on water adsorption.

704

## 705 **5. System-level screening and applications for the built environment**

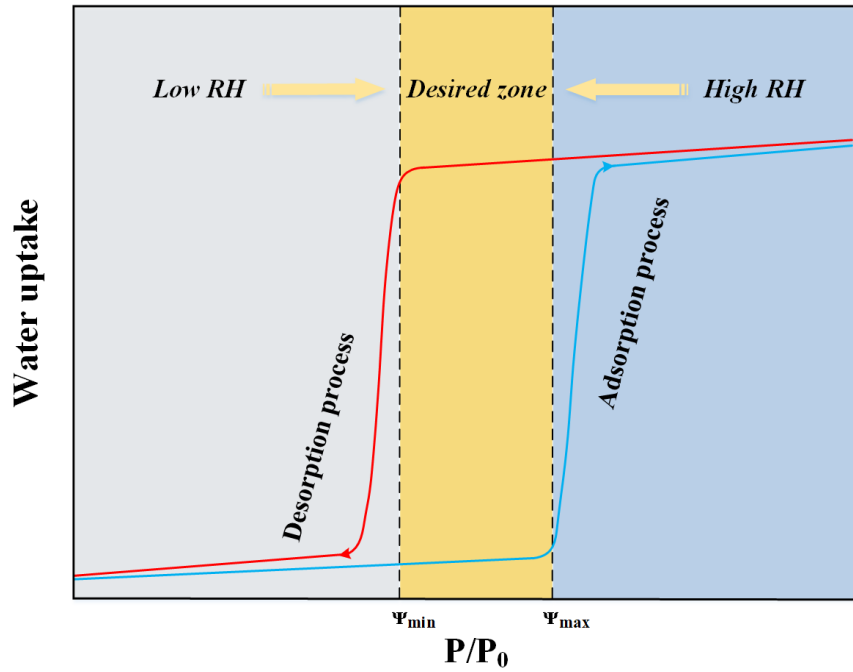
### 706 5.1. Working principles of the open solid desiccant system (SDS)

707 In general, an open SDS is designed to deal with the hygrothermal load in air, in which the  
708 desiccants directly contact with the indoor air to regulate the sensible and latent load. Open  
709 SDSs based on different working principles can be classified into active and passive types. The

710 passive-type SDS can remove the moisture fluctuation by virtue of the nature of the desiccant  
711 materials that autonomously adsorb or release the water vapor under high or low indoor  
712 humidity levels. As the intrinsic properties of the desiccant decide the operational performance,  
713 limited progress has been made in passive-type SDS systems [145-148]. As for active-type  
714 SDS, the adsorption loop forces the process air to flow through the desiccant and dehumidifies  
715 the air to the desired room temperature. The regeneration loop can reject the trapped water  
716 vapor out of the desiccant so that the desiccant can be recovered and utilized in the next  
717 operation loop. In this regard, the regeneration can be achieved by heating the desiccant to the  
718 regeneration temperature, which relies on the intrinsic properties of the desiccants (i.e. zeolite,  
719 ~100°C; MOF, 50~90°C) [11, 20, 72].

720 To date, passive-type SDS systems (Fig.20) primarily act as moisture buffer for building  
721 environment control, which contains only desiccant materials such as wood, plasterboard, etc.  
722 [149]. In contrast, active-type SDS systems (Fig.21) generally have three complex components,  
723 namely, dehumidification unit, regeneration unit and cooling unit [150]. The configuration of  
724 these units may vary largely based on the desiccant and the employed operation modes, as  
725 shown in the following section.

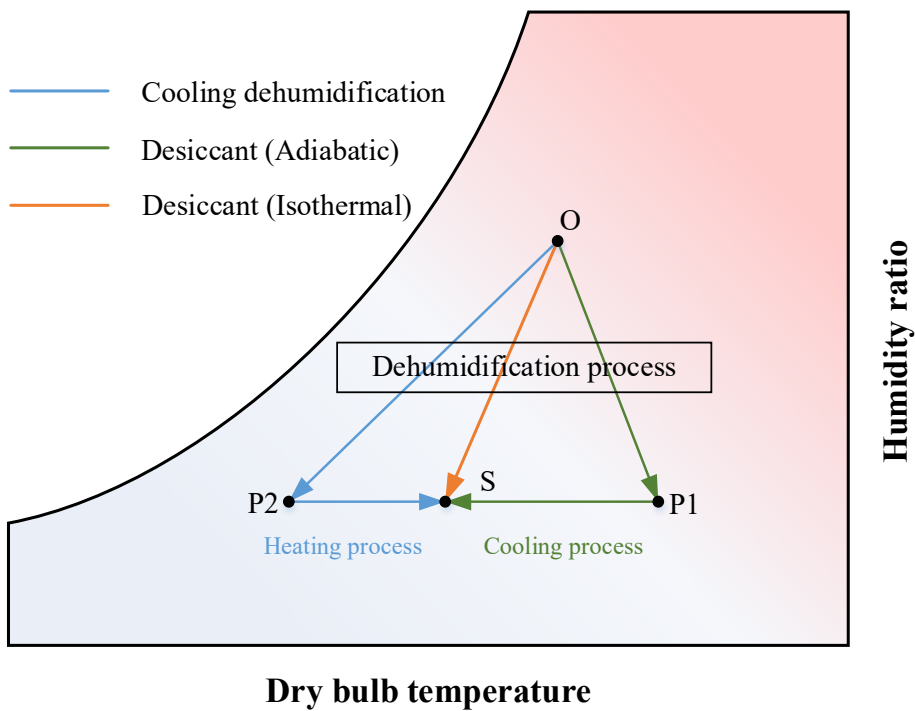
726



727

728 **Fig. 20.** The variation of water uptake in desiccant materials at high and low RH.

729



730

731 **Fig. 21.** The psychrometric processes of active-type desiccant dehumidifiers in comparison

732 with cooling dehumidification. O: outside air; S: supply air; P1 and P2: medium process.

733



734 1) Dehumidifier

735 In the case where SDS has been employed, the dehumidifier can generally work in two different  
736 manners: adiabatic [151, 152] and isothermal [9]. The process air stream directly flows through  
737 the solid desiccant in the adiabatic dehumidifiers, while in the case of isothermal dehumidifiers,  
738 the solid desiccant is not only in contact with the air stream, but is also cooled down by the  
739 cooling medium to improve the performance of desiccants. The psychrometric processes are  
740 shown in Fig.21. It is clear that the isothermal desiccant system is more desirable than the  
741 adiabatic process.

742

743 The commonly used dehumidifier types are fixed bed, rotary wheel and desiccant-coated heat  
744 exchangers (DCHEs). Since the desiccant can directly affect the performance of SDS, the  
745 selection of the desiccant for the above-mentioned systems become a focal point. Traditional  
746 desiccants such as silica gel and zeolite have been widely embedded into fixed bed [153, 154],  
747 rotary wheel [152, 155, 156] and desiccant-coated heat exchangers (DCHEs) [9, 157, 158].  
748 However, metal-organic frameworks with superior adsorption capacity and gentler  
749 regeneration condition have found little evaluation for use in dehumidifiers, thus, presenting a  
750 high potential of their application [23, 52, 159].

751

752 2) Cooling and regeneration

753 The cooling medium handles the sensible load in the cooling unit in SDS. In case an adiabatic  
754 type dehumidifier is implemented, the adsorption heat released during adsorption process  
755 gradually heats up the process air. The cooling unit can cool the air down to the desired supply  
756 air temperature. In case an isothermal type dehumidifier is employed, the cooling unit can  
757 immediately remove the adsorption heat to keep a high adsorption capacity of the desiccants.  
758 To the best of our knowledge, the common cooling unit can be a cold coil, an evaporative cooler

759 or even an evaporator in the air conditioner.

760

761 In addition, the regeneration unit in SDS is of vital significance as it supplies the thermal energy  
762 to drain the adsorbed water vapor out of the desiccants. The regenerated desiccant can therefore  
763 continue the subsequent adsorption process. As the regeneration condition is primarily decided  
764 by the intrinsic properties of the desiccants, SDS makes it possible to use a variety of energy  
765 sources, including waste heat, solar energy, electricity, etc.

766

## 767 5.2. Matching the sorption operation with the given condition

768 Based on the review on the MOF materials, it is confirmed that MOFs exhibit highly tunable  
769 structures, thus, laying promising foundation for the sorption-based humidity control. For this  
770 application, the optimal MOF materials should possess hydrothermal stability and recyclability.

771 In real life situations, air-conditioning systems usually experience multiple climate conditions  
772 during days or years. In MOF-used desiccant systems, hydrothermally stable MOFs with a  
773 steep rise in a narrow humidity range (S-shaped isotherm) are expected to maintain the  
774 humidity level during the long-term cycling operations [14]. Thus, for SDSs, the ideal MOFs  
775 for built environment control should be qualified as follows:

776

777 (1) In an active-type system, it is favorable to pick up desiccants with high water lift loading,  
778 milder regeneration condition and no or minimal hysteresis loop at the working humidity range.

779 (2) In a passive-type system, it is desirable that the hysteresis loop of the MOF desiccant formed  
780 by the adsorption-desorption branches appears during the working humidity range, and the  
781 MOF can be easily regenerated around room temperature. Moreover, these MOFs should not  
782 be temperature-sensitive, which implies that these materials are able to maintain almost the  
783 same isotherms within a certain temperature range.

784

785 In fact, many commercial and laboratory developed MOFs cannot strictly meet these  
786 requirements, especially related to hydrothermal stability. Most of heat-transformation studies  
787 on MOFs are carried out focusing on the heat pumps, adsorption-driven chillers or water  
788 harvesting etc. [23, 28, 32], however, a little knowledge is available on the open SDSs for  
789 building humidity control or the introduction of MOF-based system concept [160]. Chang et  
790 al. [78] investigated the potential of MIL-100 and MIL-101 for the energy-efficient  
791 dehumidification. Obviously, the used MOFs are promising desiccants, however, the study  
792 primarily focused on the properties of materials, rather than practical application. Lately,  
793 Henninger et al. [52] studied the MOF-coated heat exchanger at full scale considering  
794 pretreatment and coating processes. The coefficient of performance (COP) of the cooling  
795 system was estimated under different evaporator and heat rejection temperatures, and the  
796 results revealed a maximum COP up to 0.72 without heat recovery. As mentioned in the study  
797 [52], the preparation and coating processes are arduous for large-scale applications, and the  
798 recyclability of the system may need more field experiments. This work thus offers a  
799 benchmark for MOF-based open SDSs. Besides, Eddaoudi et al. [21, 42] prepared two novel  
800 desiccants with the most favorable isotherms, designed for autonomous humidity control  
801 (section 3.2.2) at room temperature. As a whole, the climate conditions, material properties and  
802 system requirements determine the design and assembly of an open SDS.

803

### 804 5.3. Alternative applications

805 The sorption-based air-conditioning system is a critical technology for achieving energy saving  
806 in building environment control. From material to system design, the selected MOFs  
807 considering the above-mentioned criteria will be integrated into a real SDS. In this context,  
808 most of currently available water-stable MOFs have been classified into three groups, and each

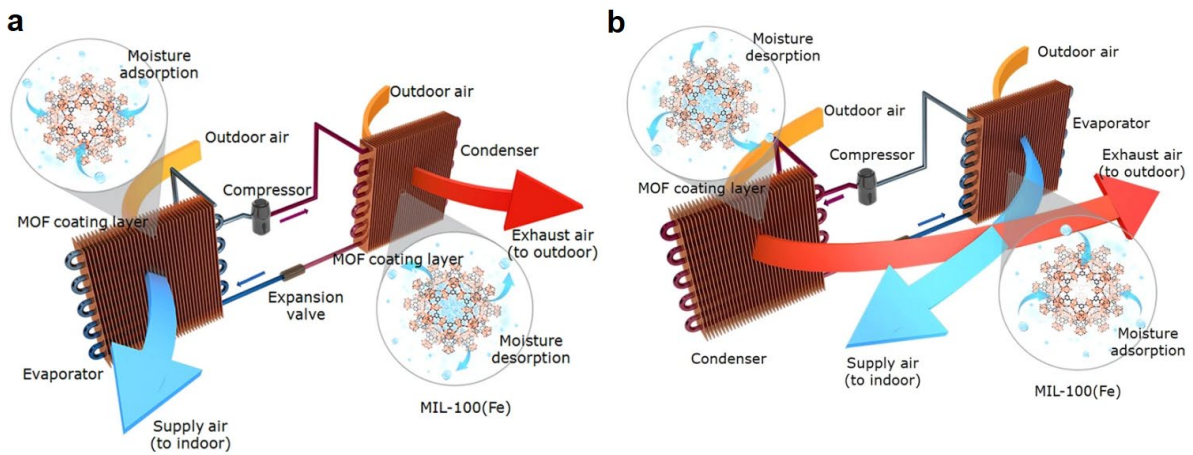
809 of these groups remains a focal point of research. It is noted that significant research efforts  
810 have been focused on the some common material properties such as water stability, water  
811 uptake capacity and regeneration of MOFs. Some other factors such as processing techniques  
812 (i.e. coating process) have been scarcely reported [52, 125, 161], which partly affect the size  
813 and performance of SDSs along with initial investment. Thus, it is needed to conduct more  
814 field measurements to assess all factors affecting MOF-based SDSs. In the following sections,  
815 we propose the case of two MOF-based systems with potential of high energy saving for the  
816 built environment control. Here, the promising candidate, MIL-100(Fe), has been applied to  
817 the systems working in active or passive mode and detailed parameters have been documented  
818 in previous studies [72, 162].

819

#### 820 5.3.1. Active system

821 Through the literature reviews on the development of sorption-based air-conditioning systems,  
822 it is clear that the traditional adiabatic dehumidification approaches (i.e. rotary wheel [152,  
823 163]) experience the severe effect of adsorption heat, which adversely reduces the total  
824 dehumidification efficiency. Therefore, a new system with desiccant-coated heat exchangers  
825 may be preferable as shown in Fig.22. The evaporator will remove the sensible load and  
826 adsorption heat to keep an isothermal adsorption, which helps to enlarge the usable water  
827 loading lift and avoid the low evaporation temperature. Although there is no heat recovery or  
828 mixing of new and exhaust air, the ultralow condensation temperature (less than 60°C) has been  
829 noted to result in COP of 7.9, which is comparable to the traditional desiccants based cooling  
830 systems [164]. As MOF is saturated in the evaporator as well as dried in the condenser,  
831 switching of the flow direction can achieve a continuous operation. Besides, the sorption  
832 kinetics confirms MIL-100(Fe) to outperform many desiccants in both adsorption rate and

833 cycling water loading. Apparently, this system can achieve a fast regulation of sensible and  
834 latent load.



835

836 **Fig. 22.** Configuration of MOF-based cooling system [72]. (a-b) The working operation of  
837 the cooling system.

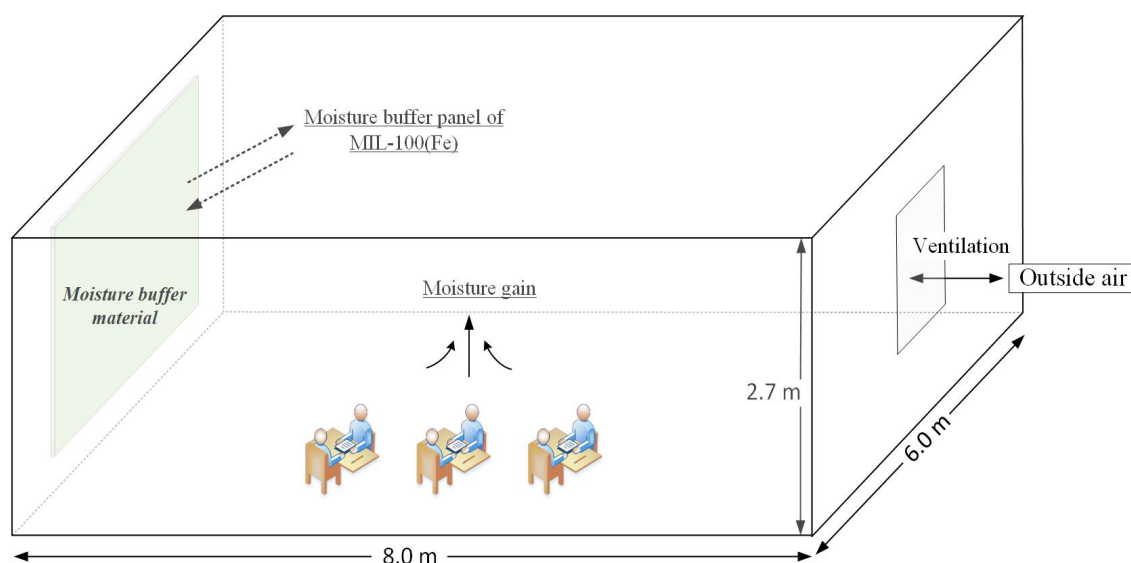
838 On the other hand, mathematical models of SDS have also been developed for several decades.  
839 To date, many research studies have been dedicated to the mathematical prediction of supply  
840 air conditioning [158, 165-167]. MOF-based model [159] has also been used recently, which  
841 helps to disclose the potential application of MOFs in the low and medium humidity  
842 environment.

843

### 844 5.3.2. Passive system

845 In 2005, Rode et al. [149] introduced a concept of moisture buffer value (MBV), which  
846 indicates that the hygroscopic materials can autonomously relieve indoor humidity fluctuation.  
847 Since then, many intensive research studies have been carried out for the model development  
848 [145, 147, 168, 169] and the assessment of buffer performance of the hygroscopic materials  
849 [170-172]. However, MBV test of the traditional hygroscopic materials such as wood, cellular  
850 concrete, etc., have been conducted on the laboratory scale, and their low moisture buffer

851 capacity indicates their inability of effective humidity control. Eddaoudi et al. [21, 42] proposed  
852 two promising MOF materials with desirable isotherms, however, these materials need more  
853 field experimental verifications at different temperature conditions. Lately, we have applied  
854 MIL-100(Fe) as a moisture buffer panel to investigate the changes in indoor humidity load at  
855 different climate conditions. The MBV ( $\sim 10 \text{ g m}^{-2} \text{ RH}\%^{-1}$ ) of MIL-100(Fe) has been measured  
856 to be one order of magnitude larger than the traditional hygroscopic material ( $\sim 1 \text{ g m}^{-2} \text{ RH}\%^{-1}$ )  
857 [162]. The configuration of the room model is shown in Fig. 23.



858

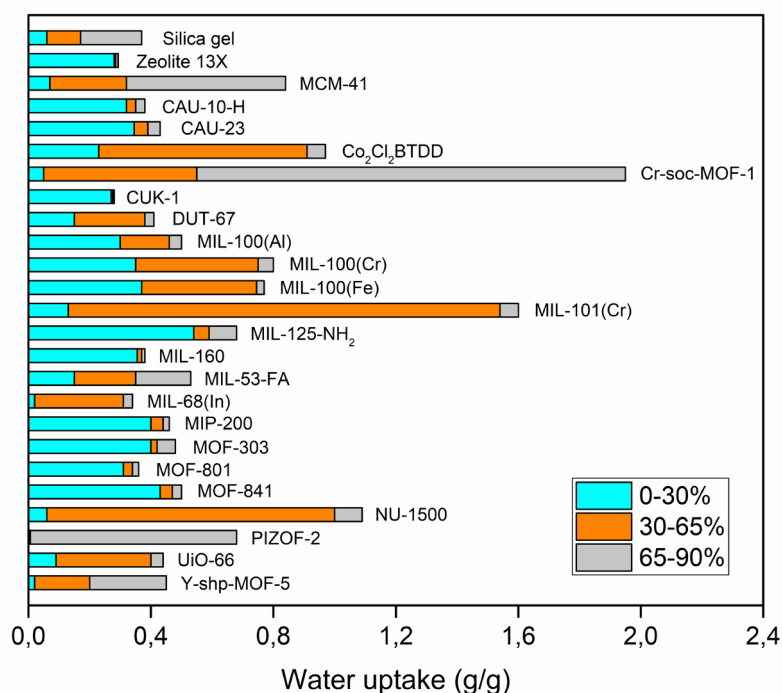
859 **Fig. 23.** The room office using a MIL-100(Fe) panel [162].

860 Considering the inner moisture gain and ventilation, the results indicate that MIL-100(Fe) can  
861 remove a majority of the latent load by night ventilation under dry and moderate climate  
862 conditions, and more than 70% of the latent load under humid climate is removed with the help  
863 of a regenerator driven by the low-grade energy such as waste heat. As the passive control of  
864 MOF-based SDSs can remove most of the latent load, it is expected that the COP of air-  
865 conditioning system will be raised without cooling dehumidification. Thus, MOFs become  
866 promising candidates as hygroscopic materials.

867

868 **6. Summary and potential**

869 Solid desiccant system is considered as a promising approach to provide a comfortable and  
 870 hygienic environment, by taking advantage of the low-grade energy. The desiccant is primarily  
 871 used to remove the latent load in a target room. Therefore, the desiccants with higher water  
 872 capacity and stable structure become potential candidates. Metal-organic frameworks (MOFs)  
 873 derived from the combination of metal clusters and organic ligands are one of the potential  
 874 categories, which possess remarkable microstructure and adsorption mechanisms, together  
 875 with structural tunability. All of the mentioned MOFs in the review fulfill the basic  
 876 requirements for SDSs, and some of them have been reported with mild regeneration conditions,  
 877 usually between 60-90°C (or even <60°C). Moreover, these MOFs with S-shaped isotherms are  
 878 also noted to outperform many traditional desiccants, as a sudden tunable change in water  
 879 uptake can take place in the working humidity range. A comprehensive comparison of the water  
 880 capacity of MOF desiccants in different pressure ranges is presented in Fig.24.



881

882 **Fig.24.** Water uptake of some representative MOFs in different relative pressure ranges.

883 In the past years, the synthesis and application of MOFs have made significant progress. The  
884 balance among the water stability, adsorption capacity and regeneration condition can be  
885 achieved through the subtle structure tailoring of the porous MOFs such as functionality or  
886 modification. The advances in the development of topology design and synthesis of MOFs [173]  
887 raise the chances of large-scale practical applications in both active and passive SDSs, and the  
888 research studies devoted to these systems are still increasing (Section 5). Despite the  
889 remarkable progresses in MOFs, no single MOF can currently meet all of the requirements  
890 owing to the drawbacks more or less related to material or system level. From the reviewed  
891 literature studies, some suggestions can be summarized as follows:

892

893 1) Chemical synthesis of MOF materials affects their intrinsic structure and material  
894 performance. The selection of green and nontoxic raw materials (metal ions, organic ligand  
895 and solvent) is preferable to produce environment-friendly MOFs [35].

896 2) Conventional synthetic methods for MOF desiccants are considered convenient, however,  
897 these may be less productive and time-consuming. Assisted synthesis [174] or flow chemistry  
898 [175] can be expected as an alternative way to produce MOFs at large scale.

899 3) The flexibility of structural tunability makes MOF remarkable intrinsic properties, which  
900 helps explain the unique water adsorption mechanisms [14].

901 4) The screening of the available MOFs based on hydrothermal stability, water adsorption and  
902 regeneration, dynamic sorption equilibrium, large-scale production and non-toxicity helps to  
903 identify the high priority of MOFs among different MOF series.

904 5) In a specific environment, open SDSs can sustain the corresponding climate change with  
905 superior recyclability. The operation in active or passive way leads to different requirements



906 for these MOF desiccants, generally focused on the shape of isotherm (i.e. hysteresis loop) and  
907 regeneration condition.

908 6) It is expected that more research studies will be available in future on the heat and mass  
909 properties of MOF desiccants, such as thermal conductivity, thermal and moisture effusivity,  
910 etc. [125]. Moreover, the applications in the desiccant-coated heat exchangers have been  
911 reported, but a little knowledge is available about the rotary wheel or fixed bed systems. In  
912 short, these properties and applications of open SDSs can prompt the use of MOF materials in  
913 built environment control.

914

915 The remarkable advances in the chemistry of MOF materials during the past years have  
916 revealed many alluring properties in comparison with the traditional solid desiccants. A  
917 systematic exploitation on the novel desiccants for SDSs is the need of the hour. In order to  
918 apply an optimal MOF to a specific SDS for the built environment control, it is essential to  
919 conduct an intensive research on the material and system levels, from structural design to  
920 material preparation, from gram scale in laboratory to ton scale in production facility, from  
921 properties assessment to system application. As some studies have confirmed that SDS using  
922 MOFs exhibits superior performance over the traditional systems, it is important to conduct  
923 further field experiments and identify the appropriate MOFs for safe, cost-effective, and energy  
924 efficient processes.

925

## 926 **Acknowledgements**

927 The authors acknowledge funding from the Chinese Scholarship Council (No. 201806230288)  
928 and the Bjarne Saxhof's Foundation.

930 **References**

- 931 [1] Lin B, Liu H. China's building energy efficiency and urbanization. *Energy Build* 2015;  
932 86: 356-365.
- 933 [2] Chua K, Chou S, Yang W, Yan J. Achieving better energy-efficient air conditioning- A  
934 review of technologies and strategies. *Appl Energy* 2013; 104: 87-104.
- 935 [3] Zhang T, Liu X, Jiang Y. Development of temperature and humidity independent  
936 control (THIC) air-conditioning systems in China- A review. *Renew Sust Energy Rev*  
937 2014; 29: 793-803.
- 938 [4] Xu X, Zhong Z, Deng S, Zhang X. A review on temperature and humidity control  
939 methods focusing on air-conditioning equipment and control algorithms applied in  
940 small-to-medium-sized buildings. *Energy Build* 2018; 162: 163-176.
- 941 [5] ASHRAE, Ventilation for Acceptable Indoor Air Quality. American Society of Heating,  
942 Refrigerating, and Air Conditioning Engineering: Atlanta, GA(US), 2010.
- 943 [6] Chaemchuen S, Xiao X, Klomkliang N, Yusubov M. Tunable metal-organic  
944 frameworks for heat transformation applications. *Nanomaterials* 2018; 8(9).
- 945 [7] Wang W, Wu L, Li Z, Fang Y, Ding J, et al. An overview of adsorbents in the rotary  
946 desiccant dehumidifier for air dehumidification. *Dry Technol* 2013; 31(12): 1334-1345.
- 947 [8] Jain S, Bansal PK. Performance analysis of liquid desiccant dehumidification systems.  
948 *Int J Refrig* 2007; 30(5): 861-872.
- 949 [9] Vivekh P, Kumja M, Bui D, Chua K. Recent developments in solid desiccant coated  
950 heat exchangers - A review. *Appl Energy* 2018; 229: 778-803.
- 951 [10] Tsobnang PK, Hastürk E, Fröhlich D, Wenger E, Durand P, et al. Water vapor single-  
952 gas selectivity via flexibility of three potential materials for autonomous indoor  
953 humidity control. *Cryst Growth Des* 2019; 19(5): 2869-2880.
- 954 [11] Zheng X, Ge TS, Wang RZ. Recent progress on desiccant materials for solid desiccant  
955 cooling systems. *Energy* 2014; 74: 280-294.
- 956 [12] Furukawa H, Cordova K, Keeffe M, Yaghi O. The chemistry and applications of metal-  
957 organic frameworks. *Science* 2013; 341(6149): 1230444.
- 958 [13] Yaghi OM, Keeffe M, Ockwig N, Chae H, Eddaoudi M, et al. Reticular synthesis and  
959 the design of new materials. *Nature* 2003; 423(6941): 705-714.
- 960 [14] Canivet J, Fateeva A, Guo Y, Coasne B, Farrusseng D. Water adsorption in MOFs:  
961 fundamentals and applications. *Chem Soc Rev* 2014; 43(16): 5594-5617.
- 962 [15] Hastürk E, Ernst SJ, Janiak C. Recent advances in adsorption heat transformation  
963 focusing on the development of adsorbent materials. *Curr Opin Chem Eng* 2019; 24:  
964 26-36.
- 965 [16] Lange MF, Verouden K, Vlugt T, Gascon J, Kapteijn F. Adsorption-driven heat pumps:  
966 The potential of metal-organic frameworks. *Chem Rev* 2015; 115(22): 12205-12250.
- 967 [17] Burtch NC, Jasuja H, Walton KS. Water stability and adsorption in metal-organic  
968 frameworks. *Chem Rev* 2014; 114(20): 10575-10612.
- 969 [18] Jeremias F, Fröhlich D, Janiak C, Henninger S. Advancement of sorption-based heat  
970 transformation by a metal coating of highly-stable, hydrophilic aluminium fumarate  
971 MOF. *RSC Adv* 2014; 4(46): 24073-24082.
- 972 [19] Fröhlich D, Pantatosaki E, Kolokathis P, Markey K, Reinsch H, et al. Water adsorption  
973 behaviour of CAU-10-H: a thorough investigation of its structure–property  
974 relationships. *J Mater Chem A* 2016; 4(30): 11859-11869.
- 975 [20] Lenzen D, Zhao J, Ernst S, Wahiduzzaman M, Inge A, et al. A metal-organic framework

- 976 for efficient water-based ultra-low-temperature-driven cooling. *Nat Commun* 2019;  
977 10(1): 3025.
- 978 [21] AbdulHalim RG, Bhatt PM, Belmabkhout Y, Shkurenko A, Adil K, et al. A fine-tuned  
979 metal-organic framework for autonomous indoor moisture control. *J Am Chem Soc*  
980 2017; 139(31): 10715-10722.
- 981 [22] Fathieh F, Kalmutzki MJ, Kapustin EA, Waller PJ, Yang JJ, et al. Practical water  
982 production from desert air. *Sci Adv* 2018; 4(6): eaat3198.
- 983 [23] Kim H, Yang S, Rao SR, Narayanan S, Kapustin EA, et al. Water harvesting from air  
984 with metal-organic frameworks powered by natural sunlight. *Science* 2017; 356(6336):  
985 430.
- 986 [24] Tu Y, Wang R, Zhang Y, Wang J. Progress and expectation of atmospheric water  
987 harvesting. *Joule* 2018; 2(8): 1452-1475.
- 988 [25] Cadiou A, Lee JS, Borges DD, Fabry P, Devic T, et al. Design of hydrophilic metal  
989 organic framework water adsorbents for heat reallocation. *Adv Mater* 2015; 27(32):  
990 4775-4780.
- 991 [26] Rieth AJ, Wright AM, Rao S, Kim H, LaPotin AD, et al. Tunable metal-organic  
992 frameworks enable high-efficiency cascaded adsorption heat pumps. *J Am Chem Soc*  
993 2018; 140(50): 17591-17596.
- 994 [27] Jeremias F, Khutia A, Henninger SK, Janiak C. MIL-100(Al, Fe) as water adsorbents  
995 for heat transformation purposes—a promising application. *J Mater Chem* 2012; 22(20):  
996 10148-10151.
- 997 [28] Khutia A, Rammelberg U, Schmidt T, Henninger S, Janiak C. Water sorption cycle  
998 measurements on functionalized MIL-101Cr for heat transformation application. *Chem*  
999 *Mater* 2013; 25(5): 790-798.
- 1000 [29] Ehrenmann J, Henninger SK, Janiak C. Water adsorption characteristics of MIL-101  
1001 for heat-transformation applications of MOFs. *Eur J of Inorg Chem* 2011; 2011(4): 471-  
1002 474.
- 1003 [30] Lee JS, Yoon JW, Mileo PGM, Cho KH, Park J, et al. Porous metal-organic framework  
1004 CUK-1 for adsorption heat allocation toward green applications of natural refrigerant  
1005 water. *ACS Appl Mater Inter* 2019; 11(29): 25778-25789.
- 1006 [31] Bon V, Senkovska I, Evans JD, Wöllner M, Hölzel M, et al. Insights into the water  
1007 adsorption mechanism in the chemically stable zirconium-based MOF DUT-67- a  
1008 prospective material for adsorption-driven heat transformations. *J Mater Chem A* 2019;  
1009 7(20): 12681-12690.
- 1010 [32] Lenzen D, Bendix P, Reinsch H, Fröhlich D, Kummer H, et al. Scalable green synthesis  
1011 and full-scale test of the metal-organic framework CAU-10-H for Use in Adsorption-  
1012 Driven Chillers. *Adv Mater* 2018; 30(6): 1705869.
- 1013 [33] Zheng J, Vemuri RS, Estevez L, Koech PK, Varga T, et al. Pore-engineered metal-  
1014 organic frameworks with excellent adsorption of water and fluorocarbon refrigerant for  
1015 cooling applications. *J Am Chem Soc* 2017; 139(31): 10601-10604.
- 1016 [34] Rezk A, Al-Dadah R, Mahmoud S, Elsayed A, et al. Characterisation of metal organic  
1017 frameworks for adsorption cooling. *Int J Heat Mass Tran* 2012; 55(25): 7366-7374.
- 1018 [35] Wang S, Serre C. Toward green production of water-stable metal-organic frameworks  
1019 based on high-valence metals with low toxicities. *ACS Sustain Chem Eng* 2019; 7(14):  
1020 11911-11927.
- 1021 [36] Wißmann G, Schaate A, Lilienthal S, Bremer I, Schneider AM, et al. Modulated  
1022 synthesis of Zr-fumarate MOF. *Micropor Mesopor Mat* 2012; 152: 64-70.
- 1023 [37] Furukawa H, Gandara F, Zhang YB, Jiang JC, Queen WL, et al. Water adsorption in  
1024 porous metal-organic frameworks and related materials. *J Am Chem Soc* 2014; 136(11):  
1025 4369-4381.

- 1026 [38] Reinsch H, Veen MAVD, B Gil, Marszalek B, Verbiest T, et al. Structures, sorption  
1027 characteristics, and nonlinear optical properties of a new series of highly stable  
1028 aluminum MOFs. *Chem Mater* 2013; 25(1): 17-26.
- 1029 [39] Rieth AJ, Yang S, Wang EN, Dincă M. Record atmospheric fresh water capture and heat  
1030 transfer with a material operating at the water uptake reversibility limit. *ACS Central*  
1031 *Sci* 2017; 3(6): 668-672.
- 1032 [40] Akiyama G, Matsuda R, Kitagawa S. Highly porous and stable coordination polymers  
1033 as water sorption materials. *Chem Lett* 2010; 39(4): 360-361.
- 1034 [41] Férey G, Mellot-Draznieks C, Serre C, Millange F, Dutour J, et al. A chromium  
1035 terephthalate-based solid with unusually large pore volumes and surface area. *Science*  
1036 2005; 309(5743): 2040.
- 1037 [42] Abtab SMT, Alezi D, Bhatt PM, Shkurenko A, Belmabkhout Y, et al. Reticular  
1038 chemistry in action: A hydrolytically stable MOF capturing twice its weight in adsorbed  
1039 water. *Chem* 2018; 4(1): 94-105.
- 1040 [43] Karmakar A, Prabakaran V, Zhao D, Chua KJ, A review of metal-organic frameworks  
1041 (MOFs) as energy-efficient desiccants for adsorption driven heat-transformation  
1042 applications. *Appl. Energy* 2020; 269: 115070.
- 1043 [44] Kalmutzki MJ, Diercks CS, Yaghi OM. Metal-organic frameworks for water harvesting  
1044 from air. *Adv Mater* 2018; 30(37): 1704304.
- 1045 [45] Küsgens P, Rose M, Senkovska I, Fröde H, Henschel A, et al. Characterization of metal-  
1046 organic frameworks by water adsorption. *Micropor Mesopor Mat* 2009; 120(3): 325-  
1047 330.
- 1048 [46] Wang S, Lee JS, Wahiduzzaman M, Park J, Muschi M, et al. A robust large-pore  
1049 zirconium carboxylate metal-organic framework for energy-efficient water-sorption-  
1050 driven refrigeration. *Nat Energy* 2018; 3(11): 985-993.
- 1051 [47] Kundu T, Sahoo SC, Banerjee R. Variable Water Adsorption in Amino Acid Derivative  
1052 Based Homochiral Metal Organic Frameworks. *Cryst Growth Des* 2012; 12(9): 4633-  
1053 4640.
- 1054 [48] Sohail M, Yun YN, Lee E, Kim SK, Cho K, et al. Synthesis of highly crystalline NH<sub>2</sub>-  
1055 MIL-125(Ti) with S-shaped water isotherms for adsorption heat transformation. *Cryst*  
1056 *Growth Des* 2017; 17(3): 1208-1213.
- 1057 [49] Bon V, Senkovska I, Baburin IA, Kaskel S. Zr- and Hf-based metal-organic frameworks:  
1058 Tracking down the polymorphism. *Cryst Growth Des* 2013; 13(3): 1231-1237.
- 1059 [50] Guo X, Zhu G, Fang Q, Xue M, Tian G, et al. Synthesis, structure and luminescent  
1060 properties of rare earth coordination polymers constructed from paddle-wheel building  
1061 blocks. *Inorg Chem* 2005; 44(11): 3850-3855.
- 1062 [51] Canivet J, Bonnefoy J, Daniel C, Legrand A, Coasne B, et al. Structure-property  
1063 relationships of water adsorption in metal-organic frameworks. *New J Chem* 2014;  
1064 38(7): 3102-3111.
- 1065 [52] Kummer H, Jeremias F, Warlo A, Földner G, Fröhlich D, et al. A functional full-scale  
1066 heat exchanger coated with aluminum fumarate metal-organic framework for  
1067 adsorption heat transformation. *Ind Eng Chem Res* 2017; 56(29): 8393-8398.
- 1068 [53] Prat D, Wells A, Hayler J, Sneddon H, McElroy CR, et al. CHEM21 selection guide of  
1069 classical- and less classical-solvents. *Green Chem* 2016; 18(1): 288-296.
- 1070 [54] Yoon JW, Seo YK, Hwang YK, Chang JS, Leclerc H, et al. Controlled reducibility of a  
1071 metal-organic framework with coordinatively unsaturated sites for preferential gas  
1072 sorption. *Angew Chem Int Edit* 2010; 49(34): 5949-5952.
- 1073 [55] Liu Y, Kabbour H, Brown CM, Neumann DA, Ahn CC. Increasing the density of  
1074 adsorbed hydrogen with coordinatively unsaturated metal centers in metal-organic  
1075 frameworks. *Langmuir* 2008; 24(9): 4772-4777.

- 1076 [56] Dietzel PDC, Johnsen RE, Blom R, Fjellvåg H, et al. Structural changes and  
1077 coordinatively unsaturated metal atoms on dehydration of honeycomb analogous  
1078 microporous metal-organic frameworks. *Chem-Eur J* 2008; 14(8): 2389-2397.
- 1079 [57] Akiyama G, Matsuda R, Sato H, Hori A, Takata M, et al. Effect of functional groups in  
1080 MIL-101 on water sorption behavior. *Micropor Mesopor Mat* 2012; 157: 89-93.
- 1081 [58] Ragon F, Campo B, Yang Q, Martineau C, Wiersum AD, et al. Acid-functionalized UiO-  
1082 66(Zr) MOFs and their evolution after intra-framework cross-linking: structural  
1083 features and sorption properties. *J Mater Chem A* 2015; 3(7): 3294-3309.
- 1084 [59] Devic T, Horcajada P, Serre C, Salles F, Maurin G, et al. Functionalization in flexible  
1085 porous solids: Effects on the pore opening and the host-guest interactions. *J Am Chem  
1086 Soc* 2010; 132(3): 1127-1136.
- 1087 [60] Juan-Alcañiz J, Gielisse R, Lago AB, Ramos-Fernandez EV, Serra-Crespo P, et al.  
1088 Towards acid MOFs-catalytic performance of sulfonic acid functionalized architectures.  
1089 *Catal Sci Technol* 2013; 3(9): 2311-2318.
- 1090 [61] Eddaoudi M, Kim J, Rosi N, Vodak D, Wachter J, et al. Systematic design of pore size  
1091 and functionality in isorecticular MOFs and their application in methane storage. *Science*  
1092 2002; 295(5554): 469.
- 1093 [62] Jasuja H, Zang J, Shollet DS, Walton KS. Rational tuning of water vapor and CO<sub>2</sub>  
1094 adsorption in highly stable Zr-based MOFs. *J Phys Chem C* 2012; 116(44): 23526-  
1095 23532.
- 1096 [63] Shi W, Zhu Y, Shen C, Shi J, Xu G, et al. Water sorption properties of functionalized  
1097 MIL-101(Cr)-X (X=-NH<sub>2</sub>, -SO<sub>3</sub>H, -H, -CH<sub>3</sub>, -F) based composites as thermochemical  
1098 heat storage materials. *Micropor Mesopor Mat* 2019; 285: 129-136.
- 1099 [64] Yan J, Yu Y, Ma C, Xiao J, Xia Q, et al. Adsorption isotherms and kinetics of water  
1100 vapor on novel adsorbents MIL-101(Cr)@GO with super-high capacity. *Appl Therm  
1101 Eng* 2015; 84: 118-125.
- 1102 [65] Yuan Y, Zhang H, Yang F, Zhang N, Cao X. Inorganic composite sorbents for water  
1103 vapor sorption: A research progress. *Renew Sustain Energy Rev* 2016; 54: 761-776.
- 1104 [66] Elsayed E, Raya ALD, Mahmoud S, Anderson P, Elsayed A. Adsorption cooling system  
1105 employing novel MIL-101(Cr)/CaCl<sub>2</sub> composites: Numerical study. *Int J Refrig* 2019;  
1106 107: 246-261.
- 1107 [67] Jabbari V, Veleta JM, Zarei-Chaleshtori M, Gardea-Torresdey J, Villagrán D. Green  
1108 synthesis of magnetic MOF@GO and MOF@CNT hybrid nanocomposites with high  
1109 adsorption capacity towards organic pollutants. *Chem Eng J* 2016; 304: 774-783.
- 1110 [68] Furukawa H, Go YB, Ko N, Park YK, Uribe-Romo FJ, et al. Isorecticular expansion of  
1111 metal-organic frameworks with triangular and square building units and the lowest  
1112 calculated density for porous crystals. *Inorg Chem* 2011; 50(18): 9147-9152.
- 1113 [69] Furukawa H, Ko N, Go YB, Aratani N, Choi SB, et al. Ultrahigh porosity in metal-  
1114 organic frameworks. *Science* 2010; 329(5990): 424.
- 1115 [70] Deng H, Grunder S, Cordova KE, Valente C, Furukawa H, et al. Large-pore apertures  
1116 in a series of metal-organic frameworks. *Science* 2012; 336(6084): 1018.
- 1117 [71] Alvarez E, Guillou N, Martineau C, Bueken B, Voorde BVD, et al. The structure of the  
1118 aluminum fumarate metal-organic framework A520. *Angew Chem Int Edit* 2015;  
1119 127(12): 3735-3739.
- 1120 [72] Cui S, Qin M, Marandi A, Steggles V, Wang S, et al. Metal-organic frameworks as  
1121 advanced moisture sorbents for energy-efficient high temperature cooling. *Sci Rep*  
1122 2018; 8(1): 15284.[73] Solovyeva MV, Gordeeva LG, Krieger TA, Aristov YI.  
1123 MOF-801 as a promising material for adsorption cooling: Equilibrium and dynamics of  
1124 water adsorption. *Energ Convers Manage* 2018; 174: 356-363.
- 1125 [74] Hanikel N, Prévot MS, Fathieh F, Kapustin EA, Lyu H, et al. Rapid cycling and

- 1126 exceptional yield in a metal-organic framework water harvester. *ACS Cent Sci* 2019; 5:  
1127 1699-1706.
- 1128 [75] Ma D, Li P, Duan X, Li J, Shao P, et al. A hydrolytically stable vanadium(IV) metal-  
1129 organic framework with photocatalytic bacteriostatic activity for autonomous indoor  
1130 humidity control. *Angew Chem Int Edit* 2020; 59: 3905-3909.
- 1131 [76] Zhang YZ, He T, Kong XJ, Lv XL, Wu XQ, et al. Tuning water sorption in highly stable  
1132 Zr(IV)-metal-organic frameworks through local functionalization of metal clusters.  
1133 *ACS Appl Mater Inter* 2018; 10(33): 27868-27874.
- 1134 [77] Ahnfeldt T, Gunzelmann D, Wack J, Senker J, Stock N. Controlled modification of the  
1135 inorganic and organic bricks in an Al-based MOF by direct and post-synthetic synthesis  
1136 routes. *CrystEngComm* 2012; 14(12): 4126-4136.
- 1137 [78] Seo YK, Yoon JW, Lee JS, Hwang YK, Jun CH, et al. Energy-efficient dehumidification  
1138 over hierarchically porous metal-organic frameworks as advanced water adsorbents.  
1139 *Adv Mater* 2012; 24(6): 806-810.
- 1140 [79] Zhang JP, Zhu AX, Lin RB, Qi XL, Chen XM. Pore surface tailored SOD-type metal-  
1141 organic zeolites. *Adv Mater* 2011; 23(10): 1268-1271.
- 1142 [80] Jeremias F, Lozan V, Henninger SK, Janiak C. Programming MOFs for water sorption:  
1143 amino-functionalized MIL-125 and UiO-66 for heat transformation and heat storage  
1144 applications. *Dalton Trans* 2013; 42(45): 15967-15973.
- 1145 [81] Luna-Triguero A, Sławek A, Huinink HP, Vlugt TJH, Poursaeidesfahani A, et al.  
1146 Enhancing the water capacity in Zr-based metal-organic framework for heat pump and  
1147 atmospheric water generator applications. *ACS Appl Nano Mater* 2019; 2(5): 3050-  
1148 3059.
- 1149 [82] Suh BL, Chong S, Kim JH. Photochemically induced water harvesting in metal-organic  
1150 framework. *ACS Sustain. Chem Eng* 2019; 7: 15854-15859.
- 1151 [83] Chen Z, Li P, Zhang X, Li P, Wasson MC, et al. Reticular access to highly porous acs-  
1152 MOFs with rigid trigonal prismatic linkers for water sorption. *J Am Chem Soc* 2019;  
1153 141(7): 2900-2905.
- 1154 [84] Schaate A, Roy P, Preuße T, Lohmeier SJ, Godt A, et al. Porous interpenetrated  
1155 zirconium-organic frameworks (PIZOFs): A chemically versatile family of metal-  
1156 organic frameworks. *Chem Eur J* 2011; 17(34): 9320-9325.
- 1157 [85] Vimont A, Goupil JM, Lavalley JC, Daturi M, Surblé S, et al. Investigation of acid sites  
1158 in a zeotypic giant pores chromium(III) carboxylate. *J Am Chem Soc* 2006; 128(10):  
1159 3218-3227.
- 1160 [86] Valenzano L, Civalleri B, Chavan S, Bordiga S, Nilsen MH, et al. Disclosing the  
1161 complex structure of UiO-66 metal organic framework: A synergic combination of  
1162 experiment and theory. *Chem Mater* 2011; 23(7): 1700-1718.
- 1163 [87] Coasne B, Galarneau A, Pellenq RJM, Renzo FD. Adsorption, intrusion and freezing in  
1164 porous silica: the view from the nanoscale. *Chem Soc Rev* 2013; 42(9): 4141-4171.
- 1165 [88] Coudert FX, Boutin A, Fuchs AH, Neimark AV. Adsorption deformation and structural  
1166 transitions in metal-organic frameworks: From the unit cell to the crystal. *J Phys Chem  
1167 Lett* 2013; 4(19): 3198-3205.
- 1168 [89] Jasuja H, Huang YG, Walton KS. Adjusting the stability of metal-organic frameworks  
1169 under humid conditions by ligand functionalization. *Langmuir* 2012; 28(49): 16874-  
1170 16880.
- 1171 [90] Taylor JM, Vaidhyanathan R, Iremonger SS, Shimizu GKH. Enhancing water stability  
1172 of metal-organic frameworks via phosphonate monoester linkers. *J Am Chem Soc* 2012;  
1173 134(35): 14338-14340.
- 1174 [91] Lv XL, Yuan S, Xie LH, Darke HF, Chen Y, et al. Ligand rigidification for enhancing  
1175 the stability of metal-organic frameworks. *J Am Chem Soc* 2019; 141(26): 10283-

- 1176 10293.
- 1177 [92] Kang IJ, Khan NA, Haque E, Jhung SH. Chemical and thermal stability of isotypic  
1178 metal-organic frameworks: Effect of metal ions. *Chem Eur J* 2011; 17(23): 6437-6442.
- 1179 [93] Bosch M, Zhang M, Zhou HC. Increasing the stability of metal-organic frameworks.  
1180 *Adv Chem* 2014; 2014: 182327.
- 1181 [94] Schoenecker PM, Carson CG, Jasuja H, Flemming CJJ, Walton KS. Effect of water  
1182 adsorption on retention of structure and surface area of metal-organic frameworks. *Ind*  
1183 *Eng Chem Res* 2012; 51(18): 6513-6519.
- 1184 [95] Low JJ, Benin AI, Jakubczak P, Abrahamian JF, Faheem SA, et al. Virtual high  
1185 throughput screening confirmed experimentally: Porous coordination polymer  
1186 hydration. *J Am Chem Soc* 2009; 131(43): 15834-15842.
- 1187 [96] DeCoste JB, Peterson GW, Jasuja H, Glover TG, Huang Y, et al. Stability and  
1188 degradation mechanisms of metal-organic frameworks containing the  $Zr_6O_4(OH)_4$   
1189 secondary building unit. *J Mater Chem A* 2013; 1(18): 5642-5650.
- 1190 [97] Cheetham AK, Kieslich G, Yeung HHM. Thermodynamic and kinetic effects in the  
1191 crystallization of metal-organic frameworks. *Acc Chem Res* 2018; 51(3): 659-667.
- 1192 [98] Guillemin V, Ragon F, Dan-Hardi M, Devic T, Vishnuvarthan M, et al. A series of  
1193 isorecticular, highly stable, porous zirconium oxide based metal-organic frameworks.  
1194 *Angew Chem Int Ed* 2012; 51(37): 9188-9188.
- 1195 [99] Liu J, Benin AI, Furtado AMB, Jakubczak P, Willis RR, et al. Stability effects on CO<sub>2</sub>  
1196 adsorption for the DOBDC series of metal-organic frameworks. *Langmuir* 2011; 27(18):  
1197 11451-11456.
- 1198 [100] Ming Y, Purewal J, Yang J, Xu C, Soltis R, et al. Kinetic stability of MOF-5 in humid  
1199 environments: Impact of powder densification, humidity level, and exposure time.  
1200 *Langmuir* 2015; 31(17): 4988-4995.
- 1201 [101] Jasuja H, et al. Kinetic Water Stability of an Isostructural Family of Zinc-Based Pillared  
1202 Metal-Organic Frameworks. *Langmuir* 2013; 29(2): 633-642.
- 1203 [102] Bon V, et al. Zr(iv) and Hf(iv) based metal-organic frameworks with reo-topology.  
1204 *Chem Commun* 2012; 48(67): 8407-8409.
- 1205 [103] Kitagawa S, Kitaura R, Noro SI. Functional porous coordination polymers. *Angew*  
1206 *Chem Int Ed* 2004; 43(18): 2334-2375.
- 1207 [104] Foley NJ, Thomas KM, Forshaw PL, Stanton D, Norman PR. Kinetics of water vapor  
1208 adsorption on activated carbon. *Langmuir* 1997; 13(7): 2083-2089.
- 1209 [105] Harding AW, Foley NJ, Norman PR, Francis DC, Thomas TK. Diffusion barriers in the  
1210 kinetics of water vapor adsorption/ desorption on activated carbons. *Langmuir* 1998;  
1211 14(14): 3858-3864.
- 1212 [106] Aristov YI, Tokarev MM, Freni A, Glaznev IS, Restuccia G. Kinetics of water  
1213 adsorption on silica Fuji Davison RD. *Micropor Mesopor Mat* 2006; 96(1): 65-71.
- 1214 [107] Hou C, Liu Q, Okamura T, Wang P, Sun WY. Dynamic porous metal-organic  
1215 frameworks: synthesis, structure and sorption property. *CrystEngComm* 2012; 14(24):  
1216 8569-8576.
- 1217 [108] Munusamy K, Sethia G, Patil DV, Rallapalli PBS, Somani RS, et al. Sorption of carbon  
1218 dioxide, methane, nitrogen and carbon monoxide on MIL-101(Cr): Volumetric  
1219 measurements and dynamic adsorption studies. *Chem Eng J* 2012; 195-196: 359-368.
- 1220 [109] Fletcher AJ, Cussen EJ, Prior TJ, Rosseinsky MJ, Kepert CJ, et al. Adsorption dynamics  
1221 of gases and vapors on the nanoporous metal organic framework material  $Ni_2(4,4'$ -  
1222  $Bipyridine)_3(NO_3)_4$ : Guest modification of host sorption behavior. *J Am Chem Soc*  
1223 2001; 123(41): 10001-10011.
- 1224 [110] Rubio-Martinez M, Avci-Camur C, Thornton AW, Imaz I, Maspocho D, et al. New  
1225 synthetic routes towards MOF production at scale. *Chem Soc Rev* 2017; 46(11): 3453-

- 1226 3480.
- 1227 [111] Dey C, Kundu T, Biswal BP, Mallick A, Banerjee R. Crystalline metal-organic  
1228 frameworks (MOFs): synthesis, structure and function. *Acta Crystallogr B* 2014; 70(1):  
1229 3-10.
- 1230 [112] Gaab M, Trukhan N, Maurer S, Gummaraju R, Müller U. The progression of Al-based  
1231 metal-organic frameworks-From academic research to industrial production and  
1232 applications. *Micropor Mesopor Mat* 2012; 157: 131-136.
- 1233 [113] Bazer-Bachi D, Assié L, Lecocq V, Harbuzaru B, Falk V. Towards industrial use of  
1234 metal-organic framework: Impact of shaping on the MOF properties. *Powder Technol*  
1235 2014; 255: 52-59.
- 1236 [114] Alvarez E, Guillou N, Martineau C, Bueken B, de Voorde BV, et al. The structure of  
1237 the aluminum fumarate metal-organic framework A520. *Angew Chem Int Ed* 2015;  
1238 54(12): 3664-3668.
- 1239 [115] Simon-Yarza T, Mielcarek A, Couvreur P, Serre C. Nanoparticles of metal-organic  
1240 frameworks: On the road to in vivo efficacy in biomedicine. *Adv Mater* 2018; 30(37):  
1241 1707365.
- 1242 [116] Reinsch H, Fröhlich D, Waitschat S, Chavan S, Lillerud KP, et al. Optimisation of  
1243 synthesis conditions for UiO-66-CO<sub>2</sub>H towards scale-up and its vapour sorption  
1244 properties. *React Chem Eng* 2018; 3(3): 365-370.
- 1245 [117] Kim H, Rao SR, Kapustin EA, Zhao L, Yang S, et al. Adsorption-based atmospheric  
1246 water harvesting device for arid climates. *Nat Commun* 2018; 9(1): 1191.
- 1247 [118] Strlič M, Thickett D, Taylor J, Cassar M. Damage functions in heritage science. *Stud*  
1248 *Conserv* 2013; 58(2): 80-87.
- 1249 [119] Fröhlich D, Henninger SK, . Janiak C. Multicycle water vapour stability of microporous  
1250 breathing MOF aluminium isophthalate CAU-10-H. *Dalton Trans* 2014; 43(41): 15300-  
1251 15304.
- 1252 [120] Waitschat S, Reinsch H, Stock N. Water-based synthesis and characterisation of a new  
1253 Zr-MOF with a unique inorganic building unit. *Chem Commun* 2016; 52(86): 12698-  
1254 12701.
- 1255 [121] Dreischarf AC, Lammert M, Stock N, Reinsch H. Green synthesis of Zr-CAU-28:  
1256 structure and properties of the first Zr-MOF based on 2,5-furandicarboxylic acid. *Inorg*  
1257 *Chem* 2017; 56(4): 2270-2277.
- 1258 [122] Waitschat S, Reinsch H, Arpacioğlu M, Stock N. Direct water-based synthesis and  
1259 characterization of new Zr/Hf-MOFs with dodecanuclear clusters as IBUs.  
1260 *CrystEngComm* 2018; 20(35): 5108-5111.
- 1261 [123] Shigematsu A, Yamada T, Kitagawa H. Wide control of proton conductivity in porous  
1262 coordination polymers. *J Am Chem Soc* 2011; 133(7): 2034-2036.
- 1263 [124] Permyakova A, Skrylnyk O, Courbon E, Affram M, Wang SJ, et al. Synthesis  
1264 optimization, shaping, and heat reallocation evaluation of the hydrophilic metal-organic  
1265 framework MIL-160(Al). *ChemSusChem* 2017; 10(7): 1419-1426.
- 1266 [125] Cui SQ, Marandi A, Lebourleux G, Thimon M, Bourdon M, et al. Heat properties of a  
1267 hydrophilic carboxylate-based MOF for water adsorption applications. *Appl Therm*  
1268 *Eng* 2019; 161: 114135.
- 1269 [126] Dan-Hardi M, Serre C, Frot T, Rozes L, Maurin G, et al. A new photoactive crystalline  
1270 highly porous titanium(IV) dicarboxylate. *J Am Chem Soc* 2009; 131(31): 10857-  
1271 10859.
- 1272 [127] Hendon CH, Tiana D, Fontecave M, Sanchez C, D'arras L, et al. Engineering the optical  
1273 response of the titanium-MIL-125 metal-organic framework through ligand  
1274 functionalization. *J Am Chem Soc* 2013; 135(30): 10942-10945.
- 1275 [128] Logan MW, Adamson JD, Le D, Uribe-Romo FJ. Structural stability of N-Alkyl-



1276 functionalized titanium metal-organic frameworks in aqueous and humid environments.  
1277 ACS Appl Mater Interfaces 2017; 9(51): 44529-44533.

1278 [129] Kim SN, Kim J, Kim HY, Cho HY, Ahn WS. Adsorption/catalytic properties of MIL-  
1279 125 and NH2-MIL-125. Catal Today 2013; 204: 85-93.

1280 [130] Wahiduzzaman M, Wang SJ, Sikora BJ, Serre C, Maurin G. Computational structure  
1281 determination of novel metal-organic frameworks. Chem Commun 2018; 54(77):  
1282 10812-10815.

1283 [131] Ahnfeldt T, Guillou N, Gunzelmann D, Margiolaki I, Loiseau T, et al.  
1284  $[Al_4(OH)_2(OCH_3)_4(H_2N-bdc)_3] \cdot x H_2O$ : A 12-connected porous metal-organic  
1285 framework with an unprecedented aluminum-containing brick. Angew Chem Int Ed  
1286 2009; 48(28): 5163-5166.

1287 [132] Dhakshinamoorthy A, Heidenreich N, Lenzen D, Stock N. Knoevenagel condensation  
1288 reaction catalysed by Al-MOFs with CAU-1 and CAU-10-type structures.  
1289 CrystEngComm 2017; 19(29): 4187-4193.

1290 [133] Reinsch H, Feyand M, Ahnfeldt T, Stock N. CAU-3: A new family of porous MOFs  
1291 with a novel Al-based brick:  $[Al_2(OCH_3)_4(O_2C-X-CO_2)]$  (X = aryl). Dalton Trans 2012;  
1292 41(14): 4164-4171.

1293 [134] Heidenreich N, Lieb A, Stock N, Reinsch H. Green synthesis of a new layered  
1294 aluminium citraconate: crystal structures, intercalation behaviour towards H<sub>2</sub>O and in  
1295 situ PXRD studies of its crystallisation. Dalton Trans 2018; 47(1): 215-223.

1296 [135] Reinsch H, Vos De D, Stock N. Structure and properties of  $[Al_4(OH)_8(o-$   
1297  $C_6H_4(CO_2)_2)_2] \cdot H_2O$ , a layered aluminum phthalate. Z Anorg Allg Chem 2013; 639(15):  
1298 2785-2789.

1299 [136] Bon V, Senkovska I, Weiss MS, Kaskel S. Tailoring of network dimensionality and  
1300 porosity adjustment in Zr- and Hf-based MOFs. CrystEngComm 2013; 15(45): 9572-  
1301 9577.

1302 [137] Férey G, Serre C, Mellot-Draznieks C, Millange F, Surblé S, et al. A hybrid solid with  
1303 giant pores prepared by a combination of targeted chemistry, simulation, and powder  
1304 diffraction. Angew Chem Int Ed 2004; 43(46): 6296-6301.

1305 [138] Henninger SK, Jeremias F, Kummer H, Janiak C. MOFs for use in adsorption heat pump  
1306 processes. Eur J Inorg Chem 2012; 2012(16): 2625-2634.

1307 [139] Wickenheisser M, Jeremias F, Henninger SK, Janiak C. Grafting of hydrophilic  
1308 ethylene glycols or ethylenediamine on coordinatively unsaturated metal sites in MIL-  
1309 100(Cr) for improved water adsorption characteristics. Inorg Chim Acta 2013; 407:  
1310 145-152.

1311 [140] Horcajada P, Surblé S, Serre C, Hong DY, Seo YK, et al. Synthesis and catalytic  
1312 properties of MIL-100(Fe), an iron(III) carboxylate with large pores. Chem Commun  
1313 2007; 27: 2820-2822.

1314 [141] Llewellyn PL, Bourrelly S, Serre C, Vimont A, Daturi M, et al. High uptakes of CO<sub>2</sub>  
1315 and CH<sub>4</sub> in mesoporous metal-organic frameworks MIL-100 and MIL-101. Langmuir  
1316 2008; 24(14): 7245-7250.

1317 [142] Wang TC, Bury W, Gómez-Gualdrón DA, Vermeulen NA, Mondloch JE, et al.  
1318 Ultrahigh surface area zirconium MOFs and insights into the applicability of the BET  
1319 theory. J Am Chem Soc 2015; 137(10): 3585-3591.

1320 [143] Farha OK, Eryazici I, Jeong NC, Hauser BG, Wilmer CE, et al. Metal-organic  
1321 framework materials with ultrahigh surface areas: Is the sky the limit? J Am Chem Soc  
1322 2012; 134(36): 15016-15021.

1323 [144] Cmarik GE, Kim M, Cohen SM, Walton KS. Tuning the adsorption properties of UiO-  
1324 66 via ligand functionalization. Langmuir 2012; 28(44): 15606-15613.

1325

- 1326 [145] Rode C, Grau K. Moisture Buffering and its Consequence in Whole Building  
1327 Hygrothermal Modeling. *J Build Phys* 2008; 31(4): 333-360.
- 1328 [146] Rode C, Peuhkuri R, Time B, Svennberg K, Ojanen T. Moisture buffer value of building  
1329 materials. *J ASTM Int* 2007; 4(5): 1-12.
- 1330 [147] Zhang M, Qin MQ, Rode C, Chen Z. Moisture buffering phenomenon and its impact  
1331 on building energy consumption. *Appl Therm Eng* 2017. 124: 337-345.
- 1332 [148] Qin M, Belarbi R, Ait-Mokhtar A, Allard F. Simulation of coupled heat and moisture  
1333 transfer in air-conditioned buildings. *Automat Constr* 2009; 18(5): 624-631.
- 1334 [149] Rode C. Moisture buffering of building materials. Department of Civil Engineering,  
1335 Technical University of Denmark, 2005.
- 1336 [150] Daou K, Wang RZ, Xia ZZ. Desiccant cooling air conditioning: a review. *Renew Sust  
1337 Energ Rev* 2006; 10(2): 55-77.
- 1338 [151] Shamim JA, Hsu WL, Kitaoka K, Paul S, Daiguji H. Design and performance  
1339 evaluation of a multilayer fixed-bed binder-free desiccant dehumidifier for hybrid air-  
1340 conditioning systems: Part I-experimental. *Int J Heat Mass Tran* 2018; 116: 1361-1369.
- 1341 [152] La D, Dai YJ, Li Y, Wang RZ, Ge TS. Technical development of rotary desiccant  
1342 dehumidification and air conditioning: A review. *Renew Sust Energ Rev* 2010; 14(1):  
1343 130-147.
- 1344 [153] Kabeel AE. Adsorption-desorption operations of multilayer desiccant packed bed for  
1345 dehumidification applications. *Renew Energ* 2009; 34(1): 255-265.
- 1346 [154] Hirunlabh J, Charoenwat R, Khedari J, Teekasap S. Feasibility study of desiccant air-  
1347 conditioning system in Thailand. *Build Environ* 2007; 42(2): 572-577.
- 1348 [155] Zhang LZ, Niu JL. Performance comparisons of desiccant wheels for air  
1349 dehumidification and enthalpy recovery. *Appl Therm Eng* 2002; 22(12): 1347-1367.
- 1350 [156] Yamaguchi S, Saito K. Numerical and experimental performance analysis of rotary  
1351 desiccant wheels. *Int J Heat Mass Tran* 2013; 60: 51-60.
- 1352 [157] Ge TS, Dai YJ, Wang RZ. Performance study of silica gel coated fin-tube heat  
1353 exchanger cooling system based on a developed mathematical model. *Energy Convers  
1354 Manag* 2011; 52(6): 2329-2338.
- 1355 [158] Jagirdar M, Lee PS. Mathematical modeling and performance evaluation of a desiccant  
1356 coated fin-tube heat exchanger. *Appl Energy* 2018; 212: 401-415.
- 1357 [159] Xu F, Bian ZF, Ge TS, Dai YJ, Wang CH, et al. Analysis on solar energy powered  
1358 cooling system based on desiccant coated heat exchanger using metal-organic  
1359 framework. *Energy* 2019; 177: 211-221.
- 1360 [160] Cao B, Tu Y, Wang RZ. A moisture-penetrating humidity pump directly powered by  
1361 one-sun illumination. *iScience* 2019; 15: 502-513.
- 1362 [161] Teo HWB, Chakraborty A, Kitagawa Y, Kayal S. Experimental study of isotherms and  
1363 kinetics for adsorption of water on aluminium fumarate. *Int J Heat Mass Tran* 2017;  
1364 114: 621-627.
- 1365 [162] Feng XX, Qin MQ, Cui SQ, Rode C. Metal-organic framework MIL-100(Fe) as a novel  
1366 moisture buffer material for energy-efficient indoor humidity control. *Build Environ*  
1367 2018; 145: 234-242.
- 1368 [163] Ge TS, Dai YJ, Wang RZ. Review on solar powered rotary desiccant wheel cooling  
1369 system. *Renew Sust Energ Rev* 2014; 39: 476-497.
- 1370 [164] Tu YD, Wang RZ, Ge TS, Zheng X. Comfortable, high-efficiency heat pump with  
1371 desiccant-coated, water-sorbing heat exchangers. *Sci Rep* 2017; 7: 40437.
- 1372 [165] Tu YD, Wang RZ, Hua LJ, Ge TS, Cao BY. Desiccant-coated water-sorbing heat  
1373 exchanger: Weakly-coupled heat and mass transfer. *Int J Heat Mass Tran* 2017; 113:  
1374 22-31.
- 1375 [166] Hua LJ, Ge TS, Wang RZ. Extremely high efficient heat pump with desiccant coated

- 1376 evaporator and condenser. *Energy* 2019; 170: 569-579.
- 1377 [167] Qin M, Belarbi R, Aït-Mokhtar A, Nilsson LO. Coupled heat and moisture transfer in  
1378 multi-layer building materials. *Constr Build Mater* 2009; 23(2): 967-975.
- 1379 [168] Abadie MO, Mendonça KC. Moisture performance of building materials: From  
1380 material characterization to building simulation using the Moisture Buffer Value  
1381 concept. *Build Environ* 2009; 44(2): 388-401.
- 1382 [169] Woods J, Winkler J, Christensen D. Evaluation of the Effective Moisture Penetration  
1383 Depth Model for Estimating Moisture Buffering in Buildings. National Renewable  
1384 Energy Lab. Golden (U.S.). 2013
- 1385 [170] Zhang H, Yoshino H, Hasegawa K. Assessing the moisture buffering performance of  
1386 hygroscopic material by using experimental method. *Build Environ* 2012; 48: 27-34.
- 1387 [171] Janssen H, Roels S. Qualitative and quantitative assessment of interior moisture  
1388 buffering by enclosures. *Energ Build* 2009; 41(4): 382-394.
- 1389 [172] Osanyintola OF, Simonson CJ. Moisture buffering capacity of hygroscopic building  
1390 materials: Experimental facilities and energy impact. *Energ Build* 2006; 38(10): 1270-  
1391 1282.
- 1392 [173] Düren T, Bae YS, Snurr RQ. Using molecular simulation to characterise metal-organic  
1393 frameworks for adsorption applications. *Chem Soc Rev* 2009; 38(5): 1237-1247.
- 1394 [174] Jhung SH, Lee JH, Yoon JW, Serre C, Férey G, et al. Microwave synthesis of chromium  
1395 terephthalate MIL-101 and its benzene sorption ability. *Adv Mater* 2007; 19(1): 121-  
1396 124.
- 1397 [175] Faustini M, Kim J, Jeong GY, Kim JY, Moon HR, et al. Microfluidic approach toward  
1398 continuous and ultrafast synthesis of metal-organic framework crystals and hetero  
1399 structures in confined microdroplets. *J Am Chem Soc* 2013; 135(39): 14619-14626.